

Abstract

We present a strategy (MIR-GBM v1.0) for the retrieval of column-averaged dry-air mole fractions of methane (X_{CH_4}) with a precision $<0.3\%$ ($1-\sigma$ diurnal variation, 7-min integration) and a seasonal bias $<0.14\%$ from mid-infrared ground-based solar FTIR measurements of the Network for the Detection of Atmospheric Composition Change (NDACC, comprising 22 FTIR stations). This makes NDACC methane data useful for satellite validation and for the inversion of regional-scale sources and sinks in addition to long-term trend analysis. Such retrievals complement the high accuracy and precision near-infrared observations of the younger Total Carbon Column Observing Network (TCCON) with time series dating back 15 yr or so before TCCON operations began.

MIR-GBM v1.0 is using HITRAN 2000 (including the 2001 update release) and 3 spectral micro windows ($2613.70\text{--}2615.40\text{ cm}^{-1}$, $2835.50\text{--}2835.80\text{ cm}^{-1}$, $2921.00\text{--}2921.60\text{ cm}^{-1}$). A first-order Tikhonov constraint is applied to the state vector given in units of per cent of volume mixing ratio. It is tuned to achieve minimum diurnal variation without damping seasonality. Final quality selection of the retrievals uses a threshold for the ratio of root-mean-square spectral residuals and information content ($<0.15\%$). Column-averaged dry-air mole fractions are calculated using the retrieved methane profiles and four-times-daily pressure-temperature-humidity profiles from National Center for Environmental Prediction (NCEP) interpolated to the time of measurement.

MIR-GBM v1.0 is the optimum of 24 tested retrieval strategies (8 different spectral micro-window selections, 3 spectroscopic line lists: HITRAN 2000, 2004, 2008). Dominant errors of the non-optimum retrieval strategies are HDO/ H_2O - CH_4 interference errors (seasonal bias up to $\approx 4\%$). Therefore interference errors have been quantified at 3 test sites covering clear-sky integrated water vapor levels representative for all NDACC sites (Wollongong maximum = 44.9 mm, Garmisch mean = 14.9 mm, Zugspitze minimum = 0.2 mm). The same quality ranking of the 24 strategies was found for all 3 test sites with one optimum, i.e., MIR-GBM v1.0.

Strategy for methane retrieval from the mid-IR FTIR network

R. Sussmann et al.

Title Page

Abstract

Introduction

Conclusions

References

Tables

Figures



Back

Close

Full Screen / Esc

Printer-friendly Version

Interactive Discussion



Seasonality of XCH₄ above the Zugspitze (47° N) shows a minus-sine shape with a minimum in March/April, a maximum in September, and an amplitude of 16.3 ± 2.9 ppb (1.0 ± 0.2 %). This agrees very well with newest-version scientific retrievals from SCIAMACHY (WFM-DOAS v2.0).

A conclusion from this paper is that improved spectroscopic parameters for CH₄, HDO, and H₂O in the 2613–2922 cm⁻¹ spectral domain are urgently needed. If such become available with sufficient accuracy, at least two more spectral micro windows could be utilized leading to another improvement in precision. The absolute intercalibration of NDACC MIR-GBM v1.0 XCH₄ to TCCON data is subject of ongoing work.

1 Introduction

Methane (CH₄) in the gas phase is characterized spectroscopically by its highly infrared active eigen modes due to the tetrahedral molecular structure. As a result, it has a global warming potential of 72 in the earth's atmosphere compared with carbon dioxide if calculated over a period of 20 yr (Forster et al., 2007). Therefore, it is the second most important anthropogenic greenhouse gas in spite of its still relatively small abundance in the atmosphere compared to carbon dioxide.

The main sources are natural wetlands, anthropogenic activities (livestock production; rice cultivation; production, storage, transmission, and distribution of fossil fuels; waste waters and landfills), and biomass burning, both natural and human-induced. About 90 % of the CH₄ loss in the atmosphere is due to the destruction by OH in the troposphere (Bousquet et al., 2011).

Methane concentrations in the atmosphere have more than doubled since begin of the industrialization and column-averaged mole fractions have reached more than 1780 ppb on a global average in 2009 (Frankenberg et al., 2011; Schneising et al., 2011). After a period of near stable concentrations at the beginning of this century, attributed to the collapse of the former USSR economy (Dlugokencky et al., 2003), the growth rate of atmospheric methane has started to increase again recently (Rigby et

Strategy for methane retrieval from the mid-IR FTIR network

R. Sussmann et al.

Title Page

Abstract

Introduction

Conclusions

References

Tables

Figures

◀

▶

◀

▶

Back

Close

Full Screen / Esc

Printer-friendly Version

Interactive Discussion



al., 2008). This increase could still be attributed to emissions from natural wetlands due to inter-annual anomalies in temperature and precipitation (Dlugokencky et al., 2009; Bousquet et al., 2011). For the future, however, there is concern that large positive feedbacks on climate warming can arise from releases of CH₄ from marine hydrates or melting permafrost.

In order to assess the effectiveness of emission reduction schemes within the frame of the Kyoto process, it is necessary to quantify the sources and sinks on the regional scale. One way to do so is the inverse modeling of atmospheric concentration measurements. This approach has recently been based upon methane surface measurements from global surface monitoring networks (Bousquet et al., 2011), or on column-averaged methane data from ENVISAT/SCIAMACHY satellite retrievals (Bergamaschi et al., 2009).

Ground-based solar FTIR measurements of methane have the potential to contribute to trend studies as well as quantification of sources and sinks. The latter can be two complementary tasks: (i) validation of satellite retrievals of methane by FTIR (e.g., Sussmann et al., 2005a; Morino et al., 2010) which is important because spatio-temporal biases of the satellite data can be misinterpreted as sources or sinks by the inversion; (ii) direct use of the ground-based FTIR network data for inverse modeling. As to (ii) it had been stated that the precision of the mid-infrared FTIR measurements of 3% and the relative accuracy of 7% at that time (2007) was significantly below the precision and (relative) accuracy targets of <1–2% of SCIAMACHY measurements (see Bergamaschi et al., 2007, and references therein). Therefore, in situ measurements of CH₄ from a comprehensive global air sampling network would be preferred since they have very high (and sufficient) precision and absolute accuracy (≈0.1%).

In situ measurements are probing the earth surface, and, therefore, additional information about the vertical distribution of CH₄ is required to render these measurements amenable for satellite validation or inverse modeling. Ground-based FTIR spectrometry, on the other hand, can directly measure the same quantity as the satellite (columns). Furthermore, measured columns contain direct information on sources and

Strategy for methane retrieval from the mid-IR FTIR network

R. Sussmann et al.

Title Page

Abstract

Introduction

Conclusions

References

Tables

Figures

◀

▶

◀

▶

Back

Close

Full Screen / Esc

Printer-friendly Version

Interactive Discussion



sinks. Thus, it could be shown that a single column-measurement station can provide significantly more information on sources and sinks than several surface stations together (Olsen and Randerson, 2004).

Column measurements for many species are performed within the Network for the Detection of Atmospheric Composition Change (NDACC, <http://www.ndacc.org>) for about two decades by ground-based solar FTIR spectrometry in the mid-infrared, currently operating with 22 NDACC FTIR stations. NDACC mid-infrared spectra have also been utilized for methane retrievals (e.g., Zander et al., 1989; Sussmann et al., 2005a; Warneke et al., 2006). These activities have recently been complemented by the Total Carbon Column Observing Network (TCCON, <http://www.tcon.caltech.edu/>) which has been designed for providing high-quality column measurements of CO₂ (and CH₄) in connection to the OCO (Orbiting Carbon Observatory) mission (Wunsch et al., 2011). TCCON is based on near-infrared solar FTIR measurements utilizing a normalization to simultaneous oxygen measurements to achieve very high precisions – for methane in the order of 0.3 % for a 1.5-min integration time (Washenfelder et al., 2003). Currently, there are 15 operational TCCON stations. Most of them began operations during the last couple of years.

It is the goal of this paper to develop a strategy to infer methane also from NDACC mid-infrared FTIR measurements with an accuracy and precision in the order of a few tenths of one per cent to make the data useful for satellite validation and for the inversion of regional-scale sources and sinks in addition to long-term trend analysis. This gives the possibility to complement the TCCON (near-infrared) observations as to spatial coverage and to provide the link to trend investigations dating back 15 yr or so before TCCON operations began.

Our paper is organized as follows. Section 2 is about the retrieval strategy. Section 2.1 describes the conceptual approach to develop the retrieval strategy and Sect. 2.2 introduces the 3 different FTIR sites used for test of the strategy. Focus is then put on selecting the best sub-set of spectral micro windows (MW) out of a candidate set of 5 MW (Sect. 2.3). Selecting the best available spectroscopic line

Strategy for methane retrieval from the mid-IR FTIR network

R. Sussmann et al.

Title Page

Abstract

Introduction

Conclusions

References

Tables

Figures



Back

Close

Full Screen / Esc

Printer-friendly Version

Interactive Discussion



Strategy for methane retrieval from the mid-IR FTIR networkR. Sussmann et al.

[Title Page](#)[Abstract](#)[Introduction](#)[Conclusions](#)[References](#)[Tables](#)[Figures](#)[◀](#)[▶](#)[◀](#)[▶](#)[Back](#)[Close](#)[Full Screen / Esc](#)[Printer-friendly Version](#)[Interactive Discussion](#)

parameters compilation is subject of Sect. 2.4: erroneous spectroscopy can lead to airmass-dependent artifacts impacting methane seasonality, as described for methane retrievals from SCIAMACHY (Frankenberg et al., 2008a). Some effort is undertaken to optimize precision for methane via a special inverse method (Sect. 2.5) and a dedicated data quality selection (Sect. 2.6). Accuracy for methane turns out to be heavily impacted by water-vapor interference errors in case a non-optimum retrieval strategy is used (Sect. 2.7). A related water-vapor-methane interference problem had been described for satellite retrievals (Frankenberg et al., 2008b). For this reason the whole study is performed using data from 3 FTIR stations (Wollongong, Garmisch, and Zugspitze) located at strongly differing climatic zones to cover all water vapor levels typical for NDACC stations. Section 2.8 shows how to calculate column-averaged dry-air mole fractions (X_{CH_4}) from the retrieved methane profiles, and Sect. 2.9 gives the final recommendation for the optimum mid-IR retrieval strategy. The X_{CH_4} seasonality is quantified for the Zugspitze site and compared to SCIAMACHY satellite data in Sect. 3. Section 4 gives the summary and an outlook.

2 Retrieval strategy and error characterization

2.1 Goal and approach

A first technical goal in optimizing the retrieval strategy is to investigate how retrievals of vertical profiles of methane can lead to improved precision for total columns compared to a simple scaling of a volume mixing ratio (vmr) profile with an altitude-constant factor. A requirement for such a profile inversion method is that it shall be based upon a robust regularization scheme that can easily be transferred to all NDACC-FTIR stations in a consistent manner. Another strategic goal is to identify a favorable selection out of five mid-IR candidate spectral micro windows (MW, see Table 1) which have been established previously within the EC project UFTIR (<http://www.nilu.no/uftir/>). Furthermore,

we want to find out which of the 3 most recent, official-release HITRAN¹ line parameters compilations (Table 1) is best suited for our mid-infrared micro windows. Finally, a concept for the quality selection of the methane retrievals shall be developed, since this is crucial to obtain a data set with optimum precision.

The conceptual approach is to perform an error characterization for multi-annual data sets prepared with varied retrieval strategies, i.e., varied subsets of the 5 candidate micro windows, and using the 3 different recent HITRAN versions for each case. A focus is on H₂O/HDO-CH₄ interference errors which turned out in the course of our study to be the dominant errors in mid-IR methane retrievals which are not carefully optimized (up to ≈4 %, for some HITRAN versions and micro-windows, see Table 4 below). Since the magnitude of the H₂O/HDO-CH₄ interference errors is expected to depend also on the overall humidity level, all test runs will be performed for data from the 3 different NDACC-FTIR sites Wollongong, Garmisch, and Zugspitze in parallel. As Table 2 shows, these test sites cover humidity levels between extremely wet to very dry due to their differing climatic locations. This range of integrated water vapor is representative for the clear-sky measurement conditions of the whole NDACC FTIR network.

2.2 FTIR measurements at 3 test sites

2.2.1 Zugspitze FTIR system

The Zugspitze (47.42° N, 10.98° E, 2964 m a.s.l.) solar FTIR system was set up in 1995 as part of the “Alpine Station” of the NDACC network. It is operated by the Group “Variability and Trends” at IMK-IFU², Karlsruhe Institute of Technology, together with a

¹ High-resolution TRANsmission molecular absorption database.

²Institute for Meteorology and Climate Research – Atmospheric Environmental Research, http://www.imk-ifu.kit.edu/atmospheric_variability.php.

Strategy for methane retrieval from the mid-IR FTIR network

R. Sussmann et al.

Title Page

Abstract

Introduction

Conclusions

References

Tables

Figures



Back

Close

Full Screen / Esc

Printer-friendly Version

Interactive Discussion



Strategy for methane retrieval from the mid-IR FTIR network

R. Sussmann et al.

Title Page

Abstract Introduction

Conclusions References

Tables Figures

◀ ▶

◀ ▶

Back Close

Full Screen / Esc

Printer-friendly Version

Interactive Discussion

variety of additional sounding systems at the Zugspitze site³. These include an AERI infrared-spectroradiometer, GPS, and two water vapor lidars (DIAL and Raman). The FTIR team contributes to satellite validation and studies of atmospheric variability and trends (e.g., Sussmann and Buchwitz, 2005; Sussmann et al., 2005a, b; Sussmann and Borsdorff, 2007; Sussmann et al., 2009; Vogelmann et al., 2011). The FTIR system is based upon a Bruker IFS 125/HR interferometer; details can be found in Sussmann and Schäfer (1997). The interferograms used for the methane retrievals have been recorded with an InSb detector using an optical path difference of typically 175 cm, averaging a number of 6 scans (≈ 7 -min integration time).

2.2.2 Garmisch FTIR system

The Garmisch solar FTIR system (47.48° N, 11.06° E, 743 m a.s.l.) was set up in 2004 and is part of the TCCON network operating in the near-infrared for high-precision retrieval of column-averaged mixing ratios of carbon dioxide and methane. The system performs mid-IR NDACC-type measurements in parallel (in alternating mode on the time scale of several minutes). The latter are utilized for this study. The system is operated together with a variety of additional sounding systems by IMK-IFU at the Garmisch site⁴, which comprises, e.g., an NDACC aerosol lidar, GPS, and an ozone lidar. The Garmisch FTIR data contribute to satellite validation and studies of atmospheric variability and trends (e.g., Morino et al., 2010; Borsdorff and Sussmann, 2009). The FTIR system is similar to the mid-IR Zugspitze set up with additional InGaAs and Si diodes (dual recording) for the near-IR measurements plus high-precision solar tracking (Bruker A547N, ± 2 min of arc) and high-accuracy pressure measurement devices. The measurement settings for the Garmisch mid-IR methane measurements are the same as detailed for the Zugspitze above.

³ Zugspitze site details can be found at <http://www.imk-ifu.kit.edu/311.php>.

⁴ Garmisch site details can be found at <http://www.imk-ifu.kit.edu/315.php>.



2.2.3 Wollongong FTIR system

The Wollongong solar FTIR system (34.45° S, 150.88° E, 35 m a.s.l.) is operated by the University of Wollongong's Center for Atmospheric Chemistry. It was setup in 1995 as part of the NDACC network. The instrument installed in 1995 was a Bomem DA8 FTIR system which operated from 1995 to 2007 (described in Griffith et al., 1998). During 2007 a Bruker IFS 125/HR instrument replaced the Bomem DA8 as part of an upgrade of the FTIR measurement program to expand the measurement capability to both the mid-IR and near-IR (Jones et al., 2011; Wunch et al., 2011). For this paper only the Bruker data were used. Spectra used for the CH₄ retrievals were obtained from interferograms recorded from an InSb detector, and a KBr beamsplitter or a CaF₂ beamsplitter. The optical path difference was 257 cm, coadding 2 consecutive interferograms giving an integration time of approximately 4 min.

2.3 Spectral information and interfering species

The spectral contributions from methane and all relevant interfering species to our candidate spectral micro windows within the measured solar absorption spectrum are plotted in Fig. 1. The most important interfering species, i.e., water vapor and its isotope HDO, can vary by factors >200 between dry NDACC sites like Zugspitze and humid sites like Wollongong, see Table 2. The spectral effect from this huge dynamic range is demonstrated in Fig. 1, see dashed versus solid lines. This provides evidence that it is important for moderate to high humidity levels to include joint fitting of HDO in all micro windows as well as joint fitting of H₂O in MW 4 and MW 5 (Table 3). Failing to perform this joint fitting of H₂O/HDO may lead to H₂O/HDO-CH₄ interference errors of the order of ≈4%. This can easily be verified from plotting the ratio of a methane column time series retrieved with and without this joint fitting as a function of HDO column level. This approach is detailed in Sect. 2.7.3 below.

Strategy for methane retrieval from the mid-IR FTIR network

R. Sussmann et al.

Title Page

Abstract

Introduction

Conclusions

References

Tables

Figures



Back

Close

Full Screen / Esc

Printer-friendly Version

Interactive Discussion



2.4 Spectroscopic line data and spectral fitting residuals

Figure 2 shows the spectral residuals (measured minus calculated) averaged over more than one year of solar absorption measurements analyzed by the non-linear least squares spectral fitting software SFIT2 (Pougatchev et al., 1995), version 3.94. The spectral residuals indicate systematic errors in the spectroscopic line data. Intriguingly, the quality of HITRAN line parameters in our 5 candidate spectral micro windows has degraded with the two updates from HITRAN 2000 (including the April 2001 update release for CH₄ and H₂O) to HITRAN 2004, and from HITRAN 2004 to HITRAN 2008. Figure 2a shows three major effects (numbers for the root-mean square of the residuals are given within the figure):

- i. HITRAN 2000 is the spectroscopy compilation with the overall smallest residuals.
- ii. The HITRAN 2004 release kept the methane line parameters in our micro windows unchanged relative to HITRAN 2000. However, HITRAN 2004 contains additional residuals due to line parameter errors for HDO in MW 4 (left hand side) and MW 5 (left hand side) as well as errors due to H₂O parameters (MW 4, right hand side, MW 5 mid to right hand side). This can be verified by comparing the residuals to the contribution plots (Fig. 1).
- iii. HITRAN 2008 shows similar problems as HITRAN 2004 for the non-methane line parameters. Additionally, the residuals due to methane have increased with HITRAN 2008. In particular, a huge error in the line strength of the 2921.33 cm⁻¹ methane line was introduced.

Figure 2b proves that HITRAN 2000 behaves comparably well for all three test sites in spite of their strongly differing humidity levels.

Strategy for methane retrieval from the mid-IR FTIR network

R. Sussmann et al.

Title Page

Abstract

Introduction

Conclusions

References

Tables

Figures

◀

▶

◀

▶

Back

Close

Full Screen / Esc

Printer-friendly Version

Interactive Discussion



2.5 Profile retrieval optimizing precision for columns

An inverse method for methane retrievals from ground-based, mid-infrared solar FTIR spectrometry has been set up via the spectral fitting software SFIT2 (Pougatchev et al., 1995), ver 3.94, which is the standard within the NDACC IRWG⁵, and is thereby easily transferable to all ground-based FTIR stations of the NDACC network.

The classical approach to retrieve total columns from ground-based FTIR spectrometry has used least squares spectral fitting with iterative scaling of an volume mixing ratio (vmr) a priori profile via one (unconstrained) altitude constant factor. This had been implemented in non-linear least squares spectral fitting software like SFIT1 (e.g., Rinsland et al., 1984) or GFIT (e.g., Toon et al., 1992). Because of the free profile scaling, this approach has the advantage that it does not damp true scaling-type columns variability in the retrieval. However, it frequently leads to significant spectral residuals. This is because of (i) likely discrepancies of the shape of the true profile relative to the a priori profile (e.g., caused by variability of the tropopause altitude) and (ii) possible spectral line shape errors in the forward calculation and/or the measurement. Both effects can introduce significant biases to the retrieved columns. A strategy to reduce this problem is to derive total columns from profile retrievals which helps to better integrate the area of the measured absorption line shape and thereby obtain a more accurate estimate of the total column integral.

Up to now, most profile retrievals from solar FTIR spectrometry have been regularized via diagonal a priori covariance matrices with the magnitude of the variances tuned empirically to avoid profile oscillations. This is sometimes referred to as “empirical implementation of optimal estimation” (e.g., Pougatchev et al., 1995). This type of profile retrieval, however, has the tendency to damp variability in the retrieved total columns as a result of profile smoothing at the cost of any deviation between the retrieved profile and the a priori profile. This damping effect is easily overlooked, and may even be misinterpreted to be an indication of good precision of the measurement.

⁵ Infrared Working Group.

Strategy for methane retrieval from the mid-IR FTIR network

R. Sussmann et al.

Title Page

Abstract

Introduction

Conclusions

References

Tables

Figures

◀

▶

◀

▶

Back

Close

Full Screen / Esc

Printer-friendly Version

Interactive Discussion



It tends to become critical in cases where the a priori covariance matrix elements are set to small values, allowing for small profile variability only and/or the retrieval contains only low information content.

Therefore, we favor a more robust retrieval that combines the advantages of both a profile scaling and a profiling approach while avoiding their disadvantages at the same time. For this purpose, we construct a regularization matrix that allows for some (constrained) flexibility in profile shape (degree of flexibility to be tuned) and also guarantees that pure profile-scaling type variations remain unconstrained. This can be achieved as follows.

The forward model \mathbf{F} maps the profiles to be retrieved from state space \mathbf{x} into measurement space \mathbf{y} . The retrieval is the (ill-posed) inverse mapping from \mathbf{y} to \mathbf{x} which is formulated as a least squares problem. Due to the non-linearity of \mathbf{F} , a Newtonian iteration is applied and a regularization term $\mathbf{R} \in \mathbb{R}^{n \times n}$ (inverse model with n layers) is used that allows one to constrain the solution and thereby avoid oscillating profiles

$$\mathbf{x}_{i+1} = \mathbf{x}_i + (\mathbf{K}_{x,i}^T \mathbf{S}_\varepsilon^{-1} \mathbf{K}_{x,i} + \mathbf{R})^{-1} \times \left\{ \mathbf{K}_{x,i}^T \mathbf{S}_\varepsilon^{-1} [\mathbf{y} - \mathbf{F}(\mathbf{x}_i)] - \mathbf{R}(\mathbf{x}_i - \mathbf{x}_a) \right\}, \quad (1)$$

where the subscript i denotes the iteration index and \mathbf{x}_a is the a priori profile. Here $\mathbf{K}_x = \partial \mathbf{F} / \partial \mathbf{x}$ are the Jacobians and \mathbf{S}_ε is the measurement covariance (assumed to be diagonal with a signal-to-rms-noise ratio of 500 in our formulation). Using first order Tikhonov regularization (Tikhonov, 1963), \mathbf{R} is set up by the relation

$$\mathbf{R} = \alpha \mathbf{L}_1^T \mathbf{L}_1 \in \mathbb{R}^{n \times n}, \quad (2)$$

where α is the regularization strength and \mathbf{L}_1 is the discrete first derivative operator

$$\mathbf{L}_1 = \begin{pmatrix} -1 & 1 & 0 & \dots & 0 \\ 0 & -1 & 1 & \ddots & \vdots \\ \vdots & \ddots & \ddots & \ddots & 0 \\ 0 & \dots & 0 & -1 & 1 \end{pmatrix} \in \mathbb{R}^{(n-1) \times n}, \quad (3)$$

Strategy for methane retrieval from the mid-IR FTIR network

R. Sussmann et al.

Title Page

Abstract

Introduction

Conclusions

References

Tables

Figures

◀

▶

◀

▶

Back

Close

Full Screen / Esc

Printer-friendly Version

Interactive Discussion



which constrains \mathbf{x} in a way such that a constant profile is favored for the difference $\mathbf{x} - \mathbf{x}_a$. The prior \mathbf{x}_a for methane and the interfering species was constructed from a multi-annual average output from the Whole Atmosphere Chemistry Climate Model (WACCM, Garcia et al., 2007), pressure-temperature profiles have been obtained from NCEP (National Center for Environmental Prediction).

Tests have shown that it is a good choice to apply the Tikhonov \mathbf{L}_1 regularization to percentage changes (or scaling factors) of the vmr of the individual profile layers to be retrieved. Another choice would be the application of \mathbf{R} to the state vector given in units of absolute vmr, which implies a differing altitude dependency of the regularization strength. An argument for the implementation of \mathbf{L}_1 in units of percentage profile changes is that this leads to the limiting case of a vmr-profile scaling, in case the regularization strength α is tuned towards infinity leading to 1 degree of freedom for signal (dofs, see Rodgers, 2000 for a definition): vmr-profile scaling is one of the best-tested retrieval approaches and well known to yield very robust retrieval results for total columns.

The details of the retrieval grid chosen impact the altitude dependency of the regularization strength. For an altitude-constant retrieval grid Eqs. (2) and (3) result in an altitude-constant regularization strength. This turned out to work robustly for water vapor (Sussmann et al., 2009) as well as for the methane retrievals and other species. In order to preserve this altitude-constant regularization in case a non-altitude constant retrieval grid is used, a transformation \mathbf{T} has to be applied to Eq. (2), i.e.,

$$\mathbf{R}' = \alpha \mathbf{L}_1^T \mathbf{T} \mathbf{L}_1, \quad (4)$$

where

$$\mathbf{T} = \begin{pmatrix} \frac{1}{\Delta z_1^2} & 0 & \dots & 0 \\ 0 & \frac{1}{\Delta z_2^2} & \ddots & \vdots \\ \vdots & \ddots & \ddots & 0 \\ 0 & \dots & 0 & \frac{1}{z_{n-1}^2} \end{pmatrix} \in \mathbb{R}^{(n-1) \times (n-1)}, \quad (5)$$

Strategy for methane retrieval from the mid-IR FTIR network

R. Sussmann et al.

Title Page

Abstract

Introduction

Conclusions

References

Tables

Figures

◀

▶

◀

▶

Back

Close

Full Screen / Esc

Printer-friendly Version

Interactive Discussion



and Δz_i is the vertical thickness of a layer with index i of the non-equidistant retrieval grid.

Finally, the regularization strength α can be optimized in a way to achieve minimum diurnal variation (optimum precision) of the retrieved CH_4 columns. Figure 3 shows that for dofs ≈ 2 a minimum for the diurnal variation can be obtained (0.23 %, 1σ). This is nearly a factor of 2 lower than the diurnal variation of 0.39 % which is obtained in case a simple vmr-profile scaling approach is used (dofs $\equiv 1$, see red point on the very left hand side of the Figure). This indicates that the optimized Tikhonov profile retrieval accounts for true profile variations in a way that helps to better integrate the measured absorption-line profile, i.e., that is closer to an equivalent width retrieval than a simple vmr-profile scaling approach. See Appendix A for ensembles of retrieved profiles and total-column averaging kernels.

Note also that the impact of using a non-ideal a priori profile upon the diurnal variation can partly be compensated by using a Tikhonov retrieval with a reduced regularization strength (higher dofs), see grey points in Fig. 3.

2.6 Quality selection

Final quality selection of the methane retrievals is crucial, e.g., for obtaining a data set of methane columns with best possible precision. Any quality selection is a trade off between improving the overall quality of the data and losing too much data. Therefore, we present an approach that optimizes this problem for ground-based FTIR spectrometry: Fig. 4a (upper trace) shows that the time series of spectral residuals bears a seasonal cycle with a maximum in winter (minimum in summer) which is due to the changing solar zenith angle. This means that a classical quality criterion using a simple threshold for the rms-residuals would eliminate more measurements in winter than in summer. However, Fig. 4a (lower trace) indicates that the information content (dofs) shows a seasonal cycle with same phase. Thus, an optimized quality criterion can be utilized using a threshold for the ratio of the spectral residuals and dofs, see Fig. 4b. Another advantage is that this threshold is more generic as it is no longer sensitive to

Strategy for methane retrieval from the mid-IR FTIR network

R. Sussmann et al.

Title Page

Abstract

Introduction

Conclusions

References

Tables

Figures



Back

Close

Full Screen / Esc

Printer-friendly Version

Interactive Discussion



the average zenith angle of a specific site. Therefore the same threshold can be used for sites at differing geographic locations. We used one common quality threshold of 0.15 % (red line in Fig. 4b) for all three test sites. This is the main quality selection rule. In addition, just to remove few obvious outliers, we added a threshold for the deviation of an individual methane-column measurement from the daily mean of <1 %.

2.7 Micro-window characterization and interference-error analysis

2.7.1 Information content

Table 4 (first rows) shows that MW 5 is the most important micro window within the set of 5 candidate MWs: excluding MW 5 leads to a stronger drop of dofs than excluding any of the other MWs. E.g., there is a drop of dofs from 1.94 to 1.75 as a result of dropping micro window 5 for Wollongong.

2.7.2 Diurnal variation

Table 4 (second rows) shows that an average precision of 0.25 % is achieved for Wollongong, 0.23 % for Garmisch, and 0.29 % for Zugspitze using all 5 candidate micro windows (precision defined as $1-\sigma$ diurnal variation for retrievals from single spectra derived from average of several scans, $\approx 4-7$ -min integration). Furthermore, the table shows that dropping individual micro windows leads to a slight increase of the diurnal variation, related to the corresponding drop in dofs. Using HITRAN 2004 or HITRAN 2008 instead of HITRAN 2000 also leads to a slight but significant increase of the diurnal variation (Table 5). In order to minimize interference errors, our final recommendation will be to use only micro windows 1, 3, and 5 together with HITRAN 2000 (see next paragraph). The resulting diurnal variations are 0.27 % for Wollongong, 0.26 % for Garmisch, and 0.30 % for Zugspitze (Table 4). This means that a precision of <0.3 % is attainable for total column methane from mid-IR NDACC-type measurements and this is comparable to the TCCON state of the art for methane of <0.3 % for single spectra.

Strategy for methane retrieval from the mid-IR FTIR network

R. Sussmann et al.

Title Page

Abstract

Introduction

Conclusions

References

Tables

Figures

◀

▶

◀

▶

Back

Close

Full Screen / Esc

Printer-friendly Version

Interactive Discussion



However, two points have to be considered for a more detailed quantitative comparison:

- i. The integration time for one single TCCON spectrum is about 1.6 min while the integration time of the mid-IR NDACC measurements of our study is ≈ 4 –7 min. Recalculating the TCCON precision for a 7-min integration would lead to $\approx 0.3\% / \sqrt{7/1.6} = 0.14\%$ which would be a factor of ≈ 2 better than the mid-IR precision of $< 0.3\%$ for total column methane.
- ii. However, in case of the mid-IR retrievals no correction for variability induced by clouds is performed, while the TCCON retrievals use a normalization by simultaneous O_2 column measurements (Washenfelder et al., 2003). The TCCON retrievals additionally include a correction for solar intensity fluctuations via the DC signal of the interferograms according to Keppel-Aleks et al. (2007). Both measures lead to a reduction of the diurnal variation (caused, e.g., by clouds), but they are applied only in case of the TCCON measurements, not in case of the mid-IR NDACC measurements.

Therefore, our interpretation of the relatively good mid-IR precision (only factor ≈ 2 lower compared to TCCON) is that both the Tikhonov profile retrieval optimized for minimum diurnal variation (Fig. 3) and the dedicated quality selection (Fig. 4) help to bring the mid-IR columnar methane retrievals' precision to this unexpected high quality level.

2.7.3 Interference errors

In the recent paper by Sussmann and Borsdorff (2007) we introduced a general formulation for a class of “interference errors” which could not be described by any of the classical four error categories of remote sounding (e.g., Rodgers, 2000, Eq. 3.16); i.e., errors in the retrieval of a target species (e.g., methane) as a result from the smoothing effect from interfering species (e.g., HDO). Additional interference effects can be due to errors in forward model parameters of the interfering species (e.g., erroneous HITRAN

Strategy for methane retrieval from the mid-IR FTIR network

R. Sussmann et al.

Title Page

Abstract

Introduction

Conclusions

References

Tables

Figures

◀

▶

◀

▶

Back

Close

Full Screen / Esc

Printer-friendly Version

Interactive Discussion



Strategy for methane retrieval from the mid-IR FTIR network

R. Sussmann et al.

Title Page

Abstract

Introduction

Conclusions

References

Tables

Figures

◀

▶

◀

▶

Back

Close

Full Screen / Esc

Printer-friendly Version

Interactive Discussion



parameters for HDO) which can be propagated into the retrieval of the target species (e.g., methane). The latter class of errors can be described by the existing concept of “(forward) model parameter errors” (second term in Rodgers, 2000, Eq. 3.16). We will hereafter present an empirical interference error analysis and, in doing so, a separation of these two differing classes of errors is neither needed nor possible. Therefore, we will use the term “interference errors” in this paper to designate either or both of the two interference phenomena.

Figure 5 shows the ratio of Garmisch year-2007 methane time series derived with two differing retrieval strategies, i.e., (i) the retrieval strategy HIT08 MW(12345) using all 5 candidate micro windows and HITRAN 2008 line parameters (which was the starting point of our study), and (ii) the retrieval strategy HIT00 MW(135) using HITRAN 2000 and using only micro windows 1, 3, and 5, which will be the final recommendation resulting from our study. The ratio time series shows a significant seasonal discrepancy between these two retrieval strategies.

The reason for this seasonal discrepancy can be understood from Fig. 6 which shows the same ratio as above as a function of the HDO column level (also for the other test sites). The HDO columns were taken from the joint HDO retrieval of the HIT00 MW(135) run. Occurrence of a strong HDO-CH₄ interference error for all test sites (up to ≈5% for Wollongong) is obvious, caused by either or both of the two retrieval strategies. HDO, together with H₂O, is the strongest interfering species in our set of 5 micro windows (Fig. 1), and the origin of the seasonal artifact of Fig. 5 can therefore be understood to be due to HDO-CH₄ (and H₂O-CH₄) interference in combination with the well know seasonal cycle of columnar HDO (like the one of H₂O, with a large-amplitude summer maximum).

We will show in the following that this interference effect is due to the HIT08 MW(12345) retrieval strategy, i.e., this interference effect can practically be eliminated by using the HIT00 MW(135) retrieval strategy. In order to show this we perform a systematic study as indicated in Fig. 7. Using HITRAN 2000 and dropping stepwise each of the 5 candidate micro windows, we quantify the resulting interference effect relative

to the HIT00 MW(12345) reference run: e.g., it can be quantified from Fig. 7d that dropping micro window 4 leads to a total relative interference error of +0.46 % which is indicated in blue in the Figure. Additionally, an overall bias of +0.27 % relative to the 5-micro window run results (indicated in red in Fig. 7d). Note, this overall bias has two major contributions in general, (i) from the average interference error (e.g., dominant contribution in Fig. 7d), and/or (ii) from methane line strength errors (e.g., dominant contribution in Fig. 7e).

Table 4 gives numbers for all the relative interference errors for all 3 test stations; e.g., for Wollongong there is a significant relative interference error upon dropping MWs 2 and 4 (+0.31 % and +0.72 %, respectively), while dropping MWs 1, 3 and 5 leads only to minor interference errors of -0.07 %, +0.10 %, and -0.17 %, respectively. Similar results are obtained for the other test stations (Table 4).

As a general result for all 3 test stations, dropping MWs 2 and 4 leads to the largest relative interference errors while dropping MWs 1, 3 and 5 leads to no significant relative interference errors. As a consequence, we will recommend later to use the HIT00 MW(135) retrieval strategy, i.e., only use micro windows number 1, 3, and 5, and drop MWs 2 and 4 as long as no better spectroscopy than HITRAN 2000 is available. (It will be shown below that HITRAN 04 and HITRAN 08 give worse results than HITRAN 2000.)

In the following we characterize the absolute quantity of the interference error of the optimum (HIT00 MW(135)) retrieval strategy; e.g., for Garmisch the HIT00 MW(135) retrieval strategy leads to a relative interference error of +0.91 % derived from the ratio series MW(135)/MW(12345) (see Table 4). We derive a twofold logical proof that this relative interference error is caused by the MW(12345) reference run – and is not due to the recommended MW(135) run – as follows: assuming that the HIT00 MW(12345) run would be absolute interference free and the relative interference error MW(135)/MW(12345) of +0.91 % would thereby be due to the HIT00 MW(135) run, the logical consequence would be that MWs 2 and 4 would cause an absolute interference error with similar magnitude but opposite sign; i.e., the relative interference error MW(24)/MW(12345) would be around $\approx -0.9\%$. This is not to be the case: according

Strategy for methane retrieval from the mid-IR FTIR network

R. Sussmann et al.

Title Page

Abstract

Introduction

Conclusions

References

Tables

Figures

◀

▶

◀

▶

Back

Close

Full Screen / Esc

Printer-friendly Version

Interactive Discussion



Strategy for methane retrieval from the mid-IR FTIR network

R. Sussmann et al.

Title Page

Abstract

Introduction

Conclusions

References

Tables

Figures

◀

▶

◀

▶

Back

Close

Full Screen / Esc

Printer-friendly Version

Interactive Discussion



to Table 4 the relative interference error $MW(24)/MW(12345)$ for Garmisch is $+0.14(8)$, i.e., in the order of $\approx 0.1\%$. This means that our starting assumption is erroneous, the absolute interference effect of the $MW(135)$ run is only in the order of $\approx 0.1\%$ and the observed relative interference effect of $+0.91\%$ is mainly due to an absolute interference error of the $MW(12345)$ run of $\approx -0.9\%$. This conclusion can be double checked by assuming the opposite, namely that the $MW(135)$ run is absolute interference free would mean that the $MW(12345)$ run would have an absolute interference error of about -0.9% caused by MWs 2 and 4. This would mean that the relative interference error $MW(24)/MW(12345)$ should be around zero. In reality it is $+0.14(8)\%$ for Garmisch (Table 4), i.e., our assumption is valid to a good approximation. In other words, the Garmisch HIT00 $MW(1235)$ run is interference free at the $\approx 0.1\%$ level.

In continuation of the previous considerations we define a way to calculate an “absolute interference error” of a certain retrieval strategy to be the negative of the sum of the relative interference errors found by dropping the different micro windows that make up this strategy; e.g., the absolute interference error for the HIT00 $MW(135)$ run would be the negative of the sum of the relative interference errors derived from the ratio time series $MW(2345)/MW(12345)$, $MW(1345)/MW(12345)$, and $MW(1234)/MW(12345)$, i.e., the absolute interference error for the Garmisch HIT00 $MW(135)$ run would be $-[(+0.01\%) + (+0.12\%) + (-0.03\%)] = -0.10\%$ (see Table 4). In an analogous absolute interference errors have been derived for Wollongong ($+0.14\%$) and for Zugspitze ($+0.2\%$). Note the improvement of these $MW(135)$ runs relative to the $MW(12345)$ runs, since the latter show an absolute interference error of -0.89% for Garmisch, -1.96% for Wollongong, and -0.35% for Zugspitze (Table 4).

It is a crucial result (from Table 4) that the quality ranking of the various retrieval strategies, according to the absolute interference error, is the same for our 3 test sites in spite of their strongly differing water vapor levels. This means that it does make sense, indeed, to recommend one joint (optimum) retrieval strategy for all NDACC sites. According to Table 4 this is the HIT00 $MW(135)$ strategy.

Strategy for methane retrieval from the mid-IR FTIR network

R. Sussmann et al.

[Title Page](#)[Abstract](#)[Introduction](#)[Conclusions](#)[References](#)[Tables](#)[Figures](#)[Back](#)[Close](#)[Full Screen / Esc](#)[Printer-friendly Version](#)[Interactive Discussion](#)

However, for a final recommendation we still have to investigate the impact of varied spectroscopy upon interference errors. All hitherto discussed results of this paper used HITRAN 2000 (Table 4). Table 5 shows the increase of interference errors upon using HITRAN 2004 or HITRAN 2008 instead. Using HITRAN 2004 leads to an unacceptable value for the absolute interference error of -3.79% for the MW(12345) run and still -3.21% for the MW(135) run. The reason behind this result that can be seen from the relative interference error of $+3.95\%$ for the HIT04 MW(1234) run. This is clearly a result of the large residual at the left hand side of MW 5 due to HDO with HITRAN 2004 (rms of 0.27% , see Fig. 2a) which is significantly larger than the residual of 0.13% with HITRAN 2000 (Fig. 2a). Also a large relative interference error from the HIT04 MW(2345) run of -0.81% arises which is caused by increased residuals in MW 1 with HITRAN 2004 compared to the case with HITRAN 2000 (Fig. 2a).

From Table 5 one might wonder whether the HIT04 MW(1234) retrieval strategy would be a reasonable alternative since the absolute interference error is $+0.16\%$, which is larger, but of the same order of magnitude of the proxy of -0.10% for the recommended HIT00 MW(135) retrieval strategy. However, the relatively small ($+0.16\%$) absolute interference error for the HIT04 MW(1234) run comprises large relative interference error components with opposite sign from the individual micro windows. These cancel out by chance, see Table 5: $-0.16\% = -0.81\%$ (from MW(2345), i.e., due to MW 1) + 0.23% (from MW(1345), i.e., due to MW 2) + 0.07% (from MW(1245), i.e., due to MW 3) + 0.35% (from MW(1235), i.e., due to MW 4). This means that the HIT04 MW(1234) retrieval strategy contains strong “internal tension”, i.e., retrievals using the individual micro windows alone, would lead to strongly differing retrieval results. This is not a recommendable, stable retrieval approach.

Finally, we investigate the use of HITRAN 2008. Similarly to HITRAN 2004, the use of HITRAN 2008 leads to an unacceptably large absolute interference error: it is -3.75% for the HIT08 MW(12345) run and still -2.75% for the HIT08 MW(135) run. The major reason for this can be seen from the relative interference error of $+3.31(9)\%$ for the HIT08 MW(1234) run which clearly is a result of the large MW-5 residual due to

the CH₄ line at 2921.33 cm⁻¹ (rms of 0.41 % see Fig. 2a), which is significantly larger than the residual of 0.27 % with HITRAN 2004 and the residual of 0.13 % with HITRAN 2000 (Fig. 2a).

Just for completeness, the HIT08 MW(1234) retrieval strategy is no alternative, since the absolute interference error for it is -0.40 % (Table 5) which is significantly larger than the value of -0.10 % achieved with our recommended HIT00 MW(135) retrieval strategy. In addition, Table 5 shows that the HIT04 MW(1234) run also comprises large relative interference error components with opposite sign from the individual micro windows (-0.64 %, +0.22 %, +0.08%, +0.74 % for MWs 1-4, respectively). This means the HIT08 MW(1234) retrieval strategy also contains strong “internal tension” – similar to what has been found for the HIT04 MW(1234) strategy.

To conclude this section, we come back to Figs. 5 and 6, which can now be understood in terms of our concepts for “relative interference error” and “absolute interference error” as follows: for Garmisch the figures show a relative interference effect for HIT08 MW(12345)/HIT00 (MW135) of ≈ -4 %. We found proof that the HIT00 MW(135) strategy is practically interference free (absolute interference error of +0.1 %, see Table 5) . From this we conclude that the absolute interference error of the HIT08 MW(12345) strategy is in the order of ≈ -4 %. This agrees with our calculated absolute interference error of -3.71 % and confirms the concept to calculate the absolute interference error from the negative of the sum of the relative interference errors.

2.8 Calculation of column-averaged dry-air mole fractions

The retrieved individual methane total columns were divided by dry air columns to obtain column-averaged dry-air mole fractions of methane (XCH₄). Dry air columns were calculated using NCEP pressure-temperature-humidity (PTU) profiles by calculating the total air column from the PT profiles and subtracting water vapor columns obtained from integrating the NCEP water vapor profiles. NCEP PTU profiles are available four times a day (06:00, 12:00, 18:00, 24:00 GMT) and were interpolated to the

Strategy for methane retrieval from the mid-IR FTIR network

R. Sussmann et al.

Title Page

Abstract

Introduction

Conclusions

References

Tables

Figures



Back

Close

Full Screen / Esc

Printer-friendly Version

Interactive Discussion



time of the FTIR measurement. This is recommended because of the strong diurnal cycle of water vapor columns above most sites.

Alternatively, information on the water vapor column can also be retrieved from the FTIR measurements. However, the water vapor retrieval is in another spectral domain than the methane retrieval. These domains are measured sequentially, not coincidentally, so that water vapor measurements may therefore not be available for all days. Additionally, an optimized water vapor retrieval has not yet been implemented by all NDACC FTIR groups. For this reason, and because comparing NECP water vapor columns to the FTIR retrievals of water vapor has shown very good agreement (Fig. 8), we favor the use of NCEP water vapor information for a harmonized NDACC retrieval strategy of methane. The FTIR retrievals of integrated water vapor used in Fig. 8 have been performed with the retrieval strategy of Sussmann et al. (2009) and have recently been inter-compared against differential absorption lidar measurements showing excellent agreement (Vogelmann et al., 2011).

2.9 Recommended retrieval strategy MIR-GBM v1.0

We make the point that it does make sense to recommend one joint mid-IR retrieval strategy for all NDACC sites. Our conclusion is based upon two findings; (i) the outcome from Sect. 2.7 that the quality ranking of the 24 differing retrieval strategies (using differing micro windows and HITRAN versions) according to the absolute $\text{H}_2\text{O}/\text{HDO}-\text{CH}_4$ interference error is the same for all three test sites of our study. (ii) The 3 test sites cover strongly differing levels of integrated water vapor which are representative of the whole NDACC network. This means we could not find any indication that there could be a retrieval strategy, optimized for the highest-humidity NDACC sites that would not also be the optimum for the driest sites.

The outcome from Sect. 2.7 (Tables 4 and 5) is that the optimum strategy for all sites is using HITRAN 2000 and micro windows 1, 3, and 5 (HIT00 MW(135)). This selection, together with our inverse method (Sect. 2.5) and the scheme for quality selection (Sect. 2.6) as well as the scheme for calculating column-averaged dry-air mole

Strategy for methane retrieval from the mid-IR FTIR network

R. Sussmann et al.

Title Page

Abstract

Introduction

Conclusions

References

Tables

Figures

◀

▶

◀

▶

Back

Close

Full Screen / Esc

Printer-friendly Version

Interactive Discussion



fractions (Sect. 2.8) comprises our new strategy for mid-IR ground-based methane retrievals. We refer to it as MIR-GBM v1.0 thereafter, see Table 7 for its definition. Table 8 gives our overall quality estimates. In another, ongoing study we perform an inter-calibration of MIR-GBM v1.0 XCH₄ to TCCON measurements. This will be subject of an upcoming publication.

3 Seasonality and comparison to SCIAMACHY data

We quantify the seasonality of XCH₄ retrieved with MIR-GBM v1.0 and compare it to SCIAMACHY data. Our motivation is threefold. (i) It is of interest to quantify and understand the true seasonality of column-averaged mole fractions of methane. This seasonality is a complex interplay between the seasonality of the emissions (most with a maximum in summer), the OH sink (maximum in summer), and the varying contribution of the stratospheric component (the tropopause altitude also shows a maximum in summer). The latter is the reason why the seasonality of XCH₄ differs from the seasonality of surface concentrations. (ii) Furthermore, we have seen in Sect. 2.7.3 that interference errors can significantly impact the retrieved seasonal cycle. Therefore, we want to validate the seasonality retrieved with our recommended retrieval strategy. (iii) Seasonalities reported from SCIAMACHY retrievals have changed over the different processor versions in amplitude and phase (Frankenberg et al., 2008a, b; Schneising et al., 2009, 2011) and it is of interest to see what the current state of the art is compared to our ground-based retrieval MIR-GBM v1.0.

Figure 9 shows the de-trended seasonality of XCH₄ derived from the Zugspitze time series. From the full Zugspitze time series covering 1995–2011 we have taken into account only the time interval between the beginning of 2004 up to the end of 2009 (2004, 2009) covering the period for which SCIAMACHY data are available. Red points in Fig. 9 are Zugspitze multi-annual monthly means for this time span. Underlying individual-year monthly means are based on 42 individual FTIR measurements on average. Since methane has shown a renewed increase during 2007–2009 after a near

Strategy for methane retrieval from the mid-IR FTIR network

R. Sussmann et al.

Title Page

Abstract

Introduction

Conclusions

References

Tables

Figures

◀

▶

◀

▶

Back

Close

Full Screen / Esc

Printer-friendly Version

Interactive Discussion



zero-trend period before (Rigby et al., 2008; Dlugokencky et al., 2009; Frankenberg et al., 2011; Schneising et al., 2011) we performed a linear de-trending for the period (2007, 2009) before calculating the multi-annual monthly means from the full (2004, 2009) interval. The de-trending was performed by the approach described in Gardiner et al. (2008).

An intra-annual function (2nd order Fourier series) was fitted to the de-trended multi-annual monthly means (red line in Fig. 9). The seasonal amplitude is 16.3 ± 2.9 ppb or $1.0 \pm 0.2\%$. The phase of the seasonality can be characterized by an approximate minus-sine-type behavior with a minimum in March/April and a maximum in September. The maxima are somewhat broader and the minima narrower than a simple sine function, however, and are described by the Fourier coefficients of Table 8 more quantitatively.

SCIAMACHY monthly mean XCH_4 data for the Northern Hemisphere retrieved with WFMD v2.0 for the years 2004–2009 were taken from Schneising et al. (2011, Fig. 12 therein). We calculated de-trended multi-annual means from this data set by the same procedure used in the FTIR data (grey line in Fig. 9). The agreement to the Zugspitze FTIR result is good. It is even better (black line) if only SCIAMACHY data for 2004–2005 are used. The reason for this is probably due to detector degradation in the spectral range used for the methane column retrieval and the corresponding availability of considerably fewer detector pixels the results, as data since November 2005 exhibit larger scatter by about a factor of two (see Fig. 12 in Schneising et al., 2011). There is good agreement both for the amplitude and the phase (see Table 8 for numbers). This indicates some breakthrough in the quality of SCIAMACHY retrievals, since earlier SCIAMACHY scientific processor versions (WFMD v1.0 or IMAP-DOAS v49) had shown a differing, “frown shape” seasonality for the Northern Hemisphere, see, e.g., Fig. 12 in Schneising et al. (2009). The reason for the much more FTIR compatible phase of the WFMD v2.0 retrievals relative to WFMD v1.0 is probably due to the use of improved methane and water vapor spectroscopy (Frankenberg et al., 2008a, b) and/or the use of an updated Carbon Tracker version (to correct the retrieved methane mole

Strategy for methane retrieval from the mid-IR FTIR network

R. Sussmann et al.

Title Page

Abstract

Introduction

Conclusions

References

Tables

Figures

◀

▶

◀

▶

Back

Close

Full Screen / Esc

Printer-friendly Version

Interactive Discussion



fractions for CO₂ seasonal variability), see Sect. 3.2 in Schneising et al. (2011) for a detailed discussion of the latter improvements.

4 Summary and outlook

4.1 Summary

5 We have developed a strategy for retrieval of atmospheric methane from mid-infrared solar absorption spectra with minimized seasonal bias <0.14% and optimized precision <0.3% (1- σ diurnal variation, 7-min integration). This optimum strategy is designated as MIR-GBM v1.0.

10 In case other, non-optimum micro window selections and/or spectroscopy selections are used, dominant errors turn out to be water vapor and HDO interference errors. Because of this finding, our study was performed in parallel with data from 3 FTIR sites (Zugspitze, Garmisch, and Wollongong) located at differing climatic zones with strongly differing mean levels of precipitable water (ranging from 0.2 mm to 44.9 mm for clear sky conditions). This is representative for the humidity levels of all NDACC sites. We
15 derived a concept for empirical estimation of the absolute interference error of a certain retrieval strategy. Performing a systematic study with 24 different retrieval strategies (8 different micro window selections and 3 different HITRAN versions) we found that the quality ranking of these 24 strategies with respect to the absolute interference error is the same for all three test sites. (Precision is only weakly impacted by the retrieval strategy.) This means that it does make sense, indeed, to agree upon one joint mid-IR
20 retrieval strategy for all NDACC sites.

The cornerstones of the recommended retrieval strategy MIR-GBM v1.0 have been summarized in Table 6. The best available spectroscopy for the mid-infrared methane retrievals is currently HITRAN 2000 including the 2001 update release. Intriguingly,
25 HITRAN 2004 and HITRAN 2008 lead to worse spectral residuals in our spectral micro windows due to line parameter errors for methane, HDO, and H₂O. However, even

Strategy for methane retrieval from the mid-IR FTIR network

R. Sussmann et al.

Title Page

Abstract

Introduction

Conclusions

References

Tables

Figures



Back

Close

Full Screen / Esc

Printer-friendly Version

Interactive Discussion



Strategy for methane retrieval from the mid-IR FTIR network

R. Sussmann et al.

Title Page

Abstract

Introduction

Conclusions

References

Tables

Figures

◀

▶

◀

▶

Back

Close

Full Screen / Esc

Printer-friendly Version

Interactive Discussion



with HITRAN 2000 it is only possible to use 3 out of 5 candidate micro windows, which would altogether be an ideal choice from a spectroscopic point of view. If more than the 3 optimum micro windows are used (first, third, fifth, if indexed for increasing wave number), significant H₂O/HDO-CH₄ interference errors up to several per cent are introduced into the retrieval. For some retrieval strategies with moderate overall interference errors strong internal “tension” is observed; i.e., there are significant interference errors due to the individual micro windows, with opposite sign. These cancel out partly in the combined multi-window retrieval. In these cases strongly differing retrieval results from stand-alone retrievals with the individual micro windows are observed. Examples of such non-recommendable retrieval strategies are those using the first 4 micro windows together with HITRAN 2004 or 2008.

The recommended retrieval constraint is the robust Tikhonov L₁ scheme set up with an altitude-constant regularization strength for a state vector given in units of per-cent of an a priori methane volume mixing ratio profile (taken from the WACCM model). The overall regularization strength is tuned in a way to achieve optimum precision (minimum diurnal variation). Thereby this high precision of <0.3% is achieved for all test sites. This is also the result of an innovative final quality selection of the retrievals utilizing not the usual threshold for the root-mean-square residual of the spectral fit but using a threshold (0.15%) for the ratio between the rms-residual and the information content (dofs) of the individual retrievals. Both quality measures show a similar zenith angle dependency, and thereby the elimination of too much data is avoided from winter when signal-to-noise is worse than in summer but information content is higher. Another benefit is that the same quality threshold can be used for all NDACC site locations with differing mean zenith angles.

Based on the retrieved total columns of methane, a method for harmonized calculation of column-averaged dry-air mole fractions (XCH₄) at all sites has been set up. It utilizes 4-times-daily information on pressure-temperature-humidity profiles from the National Center for Environmental prediction interpolated to the time of the FTIR measurement.

Strategy for methane retrieval from the mid-IR FTIR network

R. Sussmann et al.

[Title Page](#)[Abstract](#)[Introduction](#)[Conclusions](#)[References](#)[Tables](#)[Figures](#)[⏪](#)[⏩](#)[◀](#)[▶](#)[Back](#)[Close](#)[Full Screen / Esc](#)[Printer-friendly Version](#)[Interactive Discussion](#)

Finally, as stated above, due to the strong seasonality of water vapor, related interference effects potentially introduce errors in the methane seasonality, in particular for high-humidity sites. With the retrieval strategy MIR-GBM v1.0 we could eliminate H₂O/HDO-interference errors down to the <0.14% level according to our empirical interference error analysis. To double check this result we have investigated the seasonality of XCH₄ retrieved with the Zugspitze FTIR with MIR-GBM v1.0 in some detail. The outcome is a minus-sine-type seasonality with an amplitude of 16.3 ± 2.9 ppb (1.0 ± 0.2%). Comparison to newest-generation SCIAMACHY satellite retrievals (WFMD v2.0) for the Northern Hemisphere showed very good agreement in amplitude and phase.

4.2 Outlook

One outcome of this paper is that improved spectroscopic parameters for methane, HDO, and H₂O in the 2613–2922 cm⁻¹ spectral domain are urgently needed. If such parameters become available in the future, the concept for empirical interference-error quantification suggested in this paper could be applied again and our micro-window selection be repeated. This could open the possibility that all 5 of our tested candidate micro windows can be used in future. This would lead to another improvement in information content and precision compared to the current version MIR-GBM 1.0.

We were able to show that NDACC methane retrievals are possible with a precision of <0.3% for a 7-min integration time. This is only about a factor of 2 lower compared to TCCON retrievals if compared for the same integration time. This is an unexpectedly good result. Our finding, that a Tikhonov L₁ methane profile retrieval can be tuned to optimize precision, contributes to this result. It would be interesting to test this approach on TCCON retrievals as well (TCCON retrievals are hitherto based on scaling of a volume mixing ratio profile).

An inter-calibration of the absolute XCH₄ levels of the NDACC MIR-GBM v1.0 retrievals to TCCON data is subject of ongoing work and will be published elsewhere. This will be the basis for a possible joint exploitation of NDACC and TCCON data with

the potential for extended trend analyses (NDACC operations started about 15 yr before TCCON) and an improved global coverage by stations of the (joint) ground-based FTIR network for satellite validation and the inversion of sources and sinks.

Appendix A

Retrieved CH₄ profiles and averaging kernels

Figure A1 shows ensembles of retrieved methane vmr profiles using two differing micro window sets, i.e., MW(12345) (average dofs = 1.94) and MW(135) (average dofs = 1.80); HITRAN 2000 has been used in both cases. Note there is no obvious difference in profile shapes. However, what cannot be seen from this figure is that the total columns derived with the HIT00 MW(12345) retrieval strategy are significantly impacted by H₂O/HDO-CH₄ interference errors (absolute interference error = -0.86 %, see Table 5 and Sect. 2.7.3) while our recommended strategy HIT00 MW(135) is practically interference-free (absolute interference error = -0.1 %). The corresponding total-column averaging kernels are more close to uniform sampling on average for the MW(135) strategy.

Acknowledgements. We thank H. P. Schmid (IMK-IFU) for his continual interest in this work. This work has been performed as part of the ESA GHG-cci project via subcontract with University of Bremen. Earlier studies which contributed to this paper were funded by the EC within the HYMN project (contract 037048). WACCM profiles were provided by NCAR and PTU profiles by NCEP. The Wollongong work was funded through the Australian International Science Linkage grant CG130014.

Strategy for methane retrieval from the mid-IR FTIR network

R. Sussmann et al.

Title Page

Abstract

Introduction

Conclusions

References

Tables

Figures

◀

▶

◀

▶

Back

Close

Full Screen / Esc

Printer-friendly Version

Interactive Discussion



References

- Bergamaschi, P., Frankenberg, C., Meirink, J. F., Krol, M., Villani, M. G., Houweling, S., Dentener, F., Dlugokencky, E. J., Miller, J. B., Gatti, L. V., Engel, A., and Levin, I.: Inverse modeling of global and regional CH₄ emissions using SCIAMACHY satellite retrievals, *J. Geophys. Res.*, 114, D22301, doi:10.1029/2009JD012287, 2009.
- Bergamaschi, P., Frankenberg, C., Meirink, J. F., Krol, M., Dentener, F., Wagner, T., Platt, U., Kaplan, J. O., Körner, S., Heimann, M., Dlugokencky, E. J., and Goede, A.: Satellite cartography of atmospheric methane from SCIAMACHY on board ENVISAT: 2. Evaluation based on inverse model simulations, *J. Geophys. Res.*, 112, D02304, doi:10.1029/2006JD007268, 2007.
- Borsdorff, T. and Sussmann, R.: On seasonality of stratomesospheric CO above midlatitudes: New insight from solar FTIR spectrometry at Zugspitze and Garmisch, *Geophys. Res. Lett.*, 36, L21804, doi:10.1029/2009GL040056, 2009.
- Bousquet, P., Ringeval, B., Pison, I., Dlugokencky, E. J., Brunke, E.-G., Carouge, C., Chevallier, F., Fortems-Cheiney, A., Frankenberg, C., Hauglustaine, D. A., Krummel, P. B., Langenfelds, R. L., Ramonet, M., Schmidt, M., Steele, L. P., Szopa, S., Yver, C., Viovy, N., and Ciais, P.: Source attribution of the changes in atmospheric methane for 2006–2008, *Atmos. Chem. Phys.*, 11, 3689–3700, doi:10.5194/acp-11-3689-2011, 2011.
- Dlugokencky, E. J., Houweling, S., Bruhwiler, L., Masarie, K. A., Lang, P. M., Miller, J. B., and Tans, P. P.: Atmospheric methane levels off: Temporary pause or a new steady-state?, *Geophys. Res. Lett.*, 30(19), 1992, doi:10.1029/2003GL018126, 2003.
- Dlugokencky, E. J., Bruhwiler, L., White, J. W. C., Emmons, L. K., Novelli, P. C., Montzka, S. A., Masarie, K. A., Lang, P. M., Crotwell, A. M., Miller, J. B., and Gatti, L. V.: Observational constraints on recent increases in the atmospheric CH₄ burden, *Geophys. Res. Lett.*, 36, L18803, doi:10.1029/2009GL039780, 2009.
- Forster, P., Ramaswamy, V., Artaxo, P., Bernsten, T., Betts, R., Fahey, D., Haywood, J., Lean, J., Lowe, D. C., Myhre, G., Nganga, J., Prinn, R., Raga, G., Schultz, M., and Van Dorland, R.: Changes in Atmospheric Constituents and in Radiative Forcing, *Climate Change 2007: The Physical Science Basis. Contribution of Working Group I to the Fourth Assessment Report of the Intergovernmental Panel on Climate Change (IPCC)*, 2007.
- Frankenberg, C., Warneke, T., Butz, A., Aben, I., Hase, F., Spietz, P., and Brown, L. R.: Pressure broadening in the 2ν₃ band of methane and its implication on atmospheric retrievals,

AMTD

4, 2965–3015, 2011

Strategy for methane retrieval from the mid-IR FTIR network

R. Sussmann et al.

Title Page

Abstract

Introduction

Conclusions

References

Tables

Figures

◀

▶

◀

▶

Back

Close

Full Screen / Esc

Printer-friendly Version

Interactive Discussion



Strategy for methane retrieval from the mid-IR FTIR network

R. Sussmann et al.

[Title Page](#)[Abstract](#)[Introduction](#)[Conclusions](#)[References](#)[Tables](#)[Figures](#)[◀](#)[▶](#)[◀](#)[▶](#)[Back](#)[Close](#)[Full Screen / Esc](#)[Printer-friendly Version](#)[Interactive Discussion](#)

Atmos. Chem. Phys., 8, 5061–5075, doi:10.5194/acp-8-5061-2008, 2008a.

Frankenberg, C., Bergamaschi, P., Butz, A., Houweling, S., Meirink, J. F., Notholt, J., Petersen, A. K., Schrijver, H., Warneke, T., and Aben, I.: Tropical methane emissions: A revised view from SCIAMACHY onboard ENVISAT, Geophys. Res. Lett., 35, L15811, doi:10.1029/2008GL034300, 2008b.

Frankenberg, C., Aben, I., Bergamaschi, P., Dlugokencky, E. J., van Hees, R., Houweling, S., van der Meer, P., Snel, R., and Tol, P.: Global column-averaged methane mixing ratios from 2003 to 2009 as derived from SCIAMACHY: Trends and variability, J. Geophys. Res., 116, D04302, doi:10.1029/2010JD014849, 2011.

Garcia, R. R., Marsh, D. R., Kinnison, D. E., Boville, B. A., and Sassi, F.: Simulation of secular trends in the middle atmosphere, 1950–2003, J. Geophys. Res., 112, D09301, doi:10.1029/2006JD007485, 2007.

Gardiner, T., Forbes, A., de Mazière, M., Vigouroux, C., Mahieu, E., Demoulin, P., Velasco, V., Notholt, J., Blumenstock, T., Hase, F., Kramer, I., Sussmann, R., Stremme, W., Mellqvist, J., Strandberg, A., Ellingsen, K., and Gauss, M.: Trend analysis of greenhouse gases over Europe measured by a network of ground-based remote FTIR instruments, Atmos. Chem. Phys., 8, 6719–6727, doi:10.5194/acp-8-6719-2008, 2008.

Griffith, D. W. T., Jones, N. B., and Matthews, W. A.: Interhemispheric ratio and Annual Cycle of Carbonyl Sulphide (OCS) Total Column from Ground-Based FTIR Spectra, J. Geophys. Res., 103, 8447–8454, 1998.

Jones, N. B., Griffith, D. W. T., Murphy, C., Wilson, S., Deutscher, N. M., and Macatangay, R.: The Australian NDACC long term ground based measurements: site description and analysis methods, Atmos. Meas. Tech. Discuss., in preparation, 2011.

Keppel-Aleks, G., Toon, G. C., Wennberg, P. O., and Deutscher, N. M.: Reducing the impact of source brightness fluctuations on spectra obtained by Fourier-transform spectrometry, Appl. Optics, 46, 4774–4779, 2007.

Morino, I., Uchino, O., Inoue, M., Yoshida, Y., Yokota, T., Wennberg, P. O., Toon, G. C., Wunch, D., Roehl, C. M., Notholt, J., Warneke, T., Messerschmidt, J., Griffith, D. W. T., Deutscher, N. M., Sherlock, V., Connor, B., Robinson, J., Sussmann, R., and Rettinger, M.: Preliminary validation of column-averaged volume mixing ratios of carbon dioxide and methane retrieved from GOSAT short-wavelength infrared spectra, Atmos. Meas. Tech. Discuss., 3, 5613–5643, doi:10.5194/amtd-3-5613-2010, 2010.

Strategy for methane retrieval from the mid-IR FTIR network

R. Sussmann et al.

Title Page

Abstract

Introduction

Conclusions

References

Tables

Figures

◀

▶

◀

▶

Back

Close

Full Screen / Esc

Printer-friendly Version

Interactive Discussion



Olsen, S. C. and Randerson, J. T.: Differences between surface and column atmospheric CO₂ and implications for carbon cycle research, *J. Geophys. Res.*, 109, D02301, doi:10.1029/2003JD003968, 2004.

Pougatchev, N. S., Connor, B. J., and Rinsland, C. P.: Infrared measurements of the ozone vertical distribution above Kitt Peak, *J. Geophys. Res.*, 100, 16689–16697, 1995.

Rigby, M., Prinn, R. G., Fraser, P. J., Simmonds, P. G., Langenfelds, R. L., Huang, J., Cunnold, D. M., Steele, L. P., Krummel, P. B., Weiss, R. F., O'Doherty, S., Salameh, P. K., Wang, H. J., Harth, C. M., Mühle, J., and Porter, L. W.: Renewed growth of atmospheric methane, *Geophys. Res. Lett.*, 35, L22805, doi:10.1029/2008GL036037, 2008.

Rinsland, C. P., Boughner, R. E., Larsen, J. C., Stokes, G. M., and Brault, J. W.: Diurnal variations of atmospheric nitric oxide: ground-based infrared spectroscopic measurements and their interpretation with time dependent photochemical model calculations, *J. Geophys. Res.*, 89, 9613–9622, 1984.

Rodgers, C. D.: Inverse Methods for Atmospheric Sounding: Theory and Practice, vol. 2 of Series on Atmospheric, in: *Oceanic and Planetary Physics*, edited by: Taylor, F. W., World Scientific, 2000.

Rothmann, L. S., Barbe, A., Benner, D. C., Brown, L. R., Camy-Peyret, C., Carleer, M. R., Chance, K., Clerbaux, C., Dana, V., Devi, V. M., Fayt, A., Flaud, J. M., Gamache, R. R., Goldman, A., Jacquemart, D., Jucks, K. W., Lafferty, W. J., Mandin, J. Y., Massie, S. T., Nemtchinov, V., Newnham, D. A., Perrin, A., Rinsland, C. P., Schroeder, J., Smith, K. M., Smith, M. A. H., Tang, K., Toth, R. A., Vander Auwera, J., Varanasi, P., and Yoshino, K.: The HITRAN molecular spectroscopic database: edition of 2000 including updates through 2001, *J. Quant. Spectrosc. Ra.*, 82, 5–44, 2003.

Rothman, L. S., Jacquemart, D., Barbe, A., Benner, D. C., Birk, M., Brown, L. R., Carleer, M. R., Chackerian Jr., C., Chance, K., Coudert, L. H., Dana, V., Devi, V. M., Flaud, J.-M., Gamache, R. R., Goldman, A., Hartmann, J.-M., Jucks, K. W., Maki, A. G., Mandin, J.-Y., Massie, S. T., Orphal, J., Perrin, A., Rinsland, C. P., Smith, M. A. H., Tennyson, J., Tolchenov, R. N., Toth, R. A., Vander Auwera, J., Varanasi, P., and Wagner, G.: The HITRAN 2004 molecular spectroscopic database, *J. Quant. Spectrosc. Ra.*, 96, 139–204, 2005.

Rothman, L. S., Gordon, I. E., Barbe, A., Benner, D. C., Bernath, P. F., Birk, M., Boudon, V., Brown, L. R., Campargue, A., Champion, J., Chance, K., Coudert, L. H., Dana, V., Devi, V. M., Fally, S., Flaud, J. M., Gamache, R. R., Goldman, A., Jacquemart, D., Kleiner, I., Lacome, N., Lafferty, W. J., Mandin, J., Massie, S. T., Mikhailenko, S. N., Miller, C. E.,

Strategy for methane retrieval from the mid-IR FTIR network

R. Sussmann et al.

Title Page

Abstract

Introduction

Conclusions

References

Tables

Figures



Back

Close

Full Screen / Esc

Printer-friendly Version

Interactive Discussion



Moazzen-Ahmadi, N., Naumenko, O. V., Nikitin, A. V., Orphal, J., Perevalov, V. I., Perrin, A., Predoi-Cross, A., Rinsland, C. P., Rotger, M., Šimečková, M., Smith, M. A. H., Sung, K., Tashkun, S. A., Tennyson, J., Toth, R. A., Vandaele, A. C., and Vander Auwera, J.: The HITRAN 2008 molecular spectroscopic database, *J. Quant. Spectrosc. Ra.*, 110, 533–572, 2009.

Schneising, O., Buchwitz, M., Burrows, J. P., Bovensmann, H., Bergamaschi, P., and Peters, W.: Three years of greenhouse gas column-averaged dry air mole fractions retrieved from satellite – Part 2: Methane, *Atmos. Chem. Phys.*, 9, 443–465, doi:10.5194/acp-9-443-2009, 2009.

Schneising, O., Buchwitz, M., Reuter, M., Heymann, J., Bovensmann, H., and Burrows, J. P.: Long-term analysis of carbon dioxide and methane column-averaged mole fractions retrieved from SCIAMACHY, *Atmos. Chem. Phys.*, 11, 2863–2880, doi:10.5194/acp-11-2863-2011, 2011.

Sussmann, R. and Borsdorff, T.: Technical Note: Interference errors in infrared remote sounding of the atmosphere, *Atmos. Chem. Phys.*, 7, 3537–3557, doi:10.5194/acp-7-3537-2007, 2007.

Sussmann, R. and Buchwitz, M.: Initial validation of ENVISAT/SCIAMACHY columnar CO by FTIR profile retrievals at the Ground-Truthing Station Zugspitze, *Atmos. Chem. Phys.*, 5, 1497–1503, doi:10.5194/acp-5-1497-2005, 2005.

Sussmann, R. and Schäfer, K.: Infrared spectroscopy of tropospheric trace gases: combined analysis of horizontal and vertical column abundances, *Appl. Optics*, 36, 735–741, 1997.

Sussmann, R., Stremme, W., Buchwitz, M., and de Beek, R.: Validation of ENVISAT/SCIAMACHY columnar methane by solar FTIR spectrometry at the Ground-Truthing Station Zugspitze, *Atmos. Chem. Phys.*, 5, 2419–2429, doi:10.5194/acp-5-2419-2005, 2005a.

Sussmann, R., Stremme, W., Burrows, J. P., Richter, A., Seiler, W., and Rettinger, M.: Stratospheric and tropospheric NO₂ variability on the diurnal and annual scale: a combined retrieval from ENVISAT/SCIAMACHY and solar FTIR at the Permanent Ground-Truthing Facility Zugspitze/Garmisch, *Atmos. Chem. Phys.*, 5, 2657–2677, doi:10.5194/acp-5-2657-2005, 2005b.

Sussmann, R., Borsdorff, T., Rettinger, M., Camy-Peyret, C., Demoulin, P., Duchatelet, P., Mahieu, E., and Servais, C.: Technical Note: Harmonized retrieval of column-integrated atmospheric water vapor from the FTIR network – first examples for long-term records and

Strategy for methane retrieval from the mid-IR FTIR network

R. Sussmann et al.

[Title Page](#)[Abstract](#)[Introduction](#)[Conclusions](#)[References](#)[Tables](#)[Figures](#)[◀](#)[▶](#)[◀](#)[▶](#)[Back](#)[Close](#)[Full Screen / Esc](#)[Printer-friendly Version](#)[Interactive Discussion](#)

station trends, *Atmos. Chem. Phys.*, 9, 8987–8999, doi:10.5194/acp-9-8987-2009, 2009.

Tikhonov, A.: On the solution of incorrectly stated problems and a method of regularization, *Dokl. Akad. Nauk SSSR*, 151, 501–504, 1963.

Toon, G. C., Farmer, C. B., Schaper, P. W., Lowes, L. L., and Norton, R. H.: Composition measurements of the 1989 Arctic winter stratosphere by airborne infrared solar absorption spectroscopy, *J. Geophys. Res.*, 97, 7939–7961, 1992.

Vogelmann, H., Sussmann, R., Trickl, T., and Borsdorff, T.: Intercomparison of atmospheric water vapor soundings from the differential absorption lidar (DIAL) and the solar FTIR system on Mt. Zugspitze, *Atmos. Meas. Tech.*, 4, 835–841, doi:10.5194/amt-4-835-2011, 2011.

Warneke, T., Meirink, J. F., Bergamaschi, P., Grooß, J.-U., Notholt, J., Toon, G. C., Velasco, V., Goede, A. P. H., and Schrems, O.: Seasonal and latitudinal variation of atmospheric methane: A ground-based and ship-borne solar IR spectroscopic study, *Geophys. Res. Lett.*, 33, L14812, doi:10.1029/2006GL025874, 2006.

Washenfelder, R. A., Wennberg, P. O., and Toon, G. C.: Tropospheric methane retrieved from ground-based near-IR solar absorption spectra, *Geophys. Res. Lett.*, 30, 2226, doi:10.1029/2003GL017969, 2003.

Wunch, D., Toon, G. C., Blavier, J.-F. L., Washenfelder, R. A., Notholt, J., Connor, B. J., Griffith, D. W. T., Sherlock, V., and Wennberg, P. O.: The Total Carbon Column Observing Network, *Philos. T. R. Soc. A*, 369, 2087–2112, doi:10.1098/rsta.2010.0240, 2011.

Zander, R., Demoulin, Ph., Ehhalt, D. H., and Schmidt, U.: Secular Increase of the Vertical Column Abundance of Methane Derived from IR Solar Spectra Recorded at the Jungfraujoch Station, *J. Geophys. Res.*, 94, 11029–11039, 1989.

Strategy for methane retrieval from the mid-IR FTIR network

R. Sussmann et al.

Title Page

Abstract

Introduction

Conclusions

References

Tables

Figures

◀

▶

◀

▶

Back

Close

Full Screen / Esc

Printer-friendly Version

Interactive Discussion



Table 1. Spectral micro windows and molecular line parameters compilations investigated in this study to find an optimum retrieval strategy.

spectral micro windows (MW)	molecular line parameters compilations
MW1 2613.70–2615.40	HITRAN 2000 (HIT 00, Rothman et al., 2003) [*]
MW2 2650.60–2651.30	
MW3 2835.50–2835.80	HITRAN 2004 (HIT 04, Rothman et al., 2005)
MW4 2903.60–2904.03	
MW5 2921.00–2921.60	HITRAN 2008 (HIT 08, Rothmann et al., 2009)

^{*} HITRAN 2000 including the official April 2001 update release on CH₄ and H₂O.

Strategy for methane retrieval from the mid-IR FTIR network

R. Sussmann et al.

Table 2. Test sites of this study and corresponding range of integrated water vapor according to National Center for Environmental Prediction data selected for clear-sky days (FTIR measurement conditions).

	Wollongong (34° S, 30 m a.s.l.)	Garmisch (47° N, 743 m a.s.l.)	Zugspitze (47° N, 2964 m a.s.l.)
max H ₂ O column (mm*)	44.9	34.9	12.7
mean H ₂ O column (mm)	17.9	14.9	3.3
min H ₂ O column (mm)	6.9	1.9	0.2

* 1 mm corresponds to $3.345 \times 10^{21} \text{ cm}^{-2}$.

Title Page

Abstract

Introduction

Conclusions

References

Tables

Figures

◀

▶

◀

▶

Back

Close

Full Screen / Esc

Printer-friendly Version

Interactive Discussion



Strategy for methane retrieval from the mid-IR FTIR network

R. Sussmann et al.

Title Page

Abstract

Introduction

Conclusions

References

Tables

Figures

◀

▶

◀

▶

Back

Close

Full Screen / Esc

Printer-friendly Version

Interactive Discussion

**Table 3.** Interfering species that have to be taken into account in the 5 candidate micro windows (MW, defined in Table 1).

MW	interfering species fit (scaling)
MW 1	HDO, CO ₂
MW 2	HDO, CO ₂
MW 3	HDO
MW 4	HDO, H ₂ O, NO ₂
MW 5	HDO, H ₂ O, NO ₂

Strategy for methane retrieval from the mid-IR FTIR network

R. Sussmann et al.

[Title Page](#)

[Abstract](#) [Introduction](#)

[Conclusions](#) [References](#)

[Tables](#) [Figures](#)

[◀](#) [▶](#)

[◀](#) [▶](#)

[Back](#) [Close](#)

[Full Screen / Esc](#)

[Printer-friendly Version](#)

[Interactive Discussion](#)



Table 5. Effect from dropping individual micro windows using 3 different HITRAN versions for the test station Garmisch; impact on information content (dofs), interference errors, and diurnal variation.

micro windows used	MW (12345)	MW (2345)	MW (1345)	MW (1245)	MW (1235)	MW (1234)	MW (135)	MW (24)	
HITRAN 2000	dofs diurn. variat. ^a (%)	1.94 ±0.23	1.85 ±0.25	1.91 ±0.24	1.92 ±0.23	1.84 ±0.24	1.76 ±0.27	1.80 ±0.26	1.52 ±0.41
	rel. IF-error ^b (%)	–	+0.01(2)	+0.30(1)	+0.12(0)	+0.46(2)	–0.03(4)	+0.91(3)	+0.14(8)
	abs. IF error ^c (%)	–0.86	–0.85	–0.56	–0.74	–0.40	–0.89	–0.10	–0.76
	rel. bias ^d (%)	–	–0.18	+0.13	+0.07	+0.27	–0.27	+0.48	–1.05
	Dofs diurn. variat. ^a (%)	1.92 ±0.27	1.83 ±0.30	1.90 ±0.28	1.90 ±0.27	1.82 ±0.27	1.75 ±0.28	1.79 ±0.29	1.52 ±0.36
HITRAN 2004	rel. IF error ^b (%)	–	–0.81(3)	+0.23(1)	+0.07(0)	+0.35(2)	+3.95(5)	+0.66(3)	+3.37(8)
	abs. IF error ^c (%)	–3.79	–4.60	–3.56	–3.72	–3.44	+0.16	–3.21	–0.58
	rel. bias ^d (%)	–	–0.69	+0.09	+0.05	+0.33	+1.70	+0.49	+0.61
	Dofs diurn. variat. ^a (%)	1.92 ±0.34	1.82 ±0.39	1.89 ±0.34	1.90 ±0.34	1.81 ±0.36	1.75 ±0.28	1.77 ±0.36	1.52 ±0.37
	rel. IF error ^b (%)	–	–0.64(4)	+0.22(1)	+0.08(0)	+0.74(2)	+3.31(9)	+1.08(3)	+2.71(11)
HITRAN 2008	abs. IF error ^c (%)	–3.71	–4.35	–3.49	–3.63	–2.97	–0.40	–2.75	–0.96
	rel. bias ^d (%)	–	–0.19	+0.32	+0.12	+1.29	+0.14	+1.95	–1.31

^a Diurnal variation of individual days (1σ), averaged over all days of full time series.

^b “Relative interference error”, defined as HDO/H₂O-CH₄ interference error relative to MW(12345), see Fig. 7; uncertainties in brackets are for 95% confidence.

^c “Absolute interference error”, defined as the negative of the sum over the rel. IF errors (row above).

^d Bias rel. to MW(12345), see Fig. 7.

Strategy for methane retrieval from the mid-IR FTIR network

R. Sussmann et al.

Table 6. Optimum strategy for retrieval of methane from mid-infrared solar spectra designated as MIR-GBM v1.0.

micro windows (interfering species fitted)	2613.70–2615.40 (HDO, CO ₂) 2835.50–2835.80 (HDO) 2921.00–2921.60 (HDO, H ₂ O, NO ₂)
line list	HITRAN 2000 including 2001 update release
retrieval constraint	Tikhonov L_1
regularization strength	α tuned for minimum diurnal variation (dofs ≈ 2)
altitude dependency of reg. strength	altitude constant on per-cent-vmr scale
a priori vmr profiles	WACCM
retrieval quality selection	threshold (0.15 %) for rms-residual/dofs
calculation of column-averaged dry-air mole fractions	use 4-times-daily-NCEP PTU profiles, interpolate to FTIR measurement time, calculate air column, subtract water vapor column

Title Page

Abstract

Introduction

Conclusions

References

Tables

Figures

◀

▶

◀

▶

Back

Close

Full Screen / Esc

Printer-friendly Version

Interactive Discussion



Strategy for methane retrieval from the mid-IR FTIR network

R. Sussmann et al.

Title Page

Abstract

Introduction

Conclusions

References

Tables

Figures



Back

Close

Full Screen / Esc

Printer-friendly Version

Interactive Discussion

**Table 7.** Information on accuracy and precision for methane column-averaged dry-air mole fractions retrieved from mid-infrared solar spectra with the retrieval strategy MIR-GBM v1.0.

precision ($1-\sigma$ diurnal variation)*	<0.3 %
seasonal bias ($\text{H}_2\text{O}/\text{HDO}$ -interference error)	<0.14 %

* for 7-min integration.

Strategy for methane retrieval from the mid-IR FTIR network

R. Sussmann et al.

Title Page

Abstract

Introduction

Conclusions

References

Tables

Figures

◀

▶

◀

▶

Back

Close

Full Screen / Esc

Printer-friendly Version

Interactive Discussion



Table 8. Parameters describing the seasonality of column-averaged mole fractions of methane.

	amplitude ^a	phase	Fourier components ^b
Zugspitze FTIR ^c			
47° N, 11° E	16.3 ± 2.9 ppb ^d or 1.0 ± 0.2 %	min: March/April max: Sep “minus-sine type”	$a_1 = -5.5$ ppb $a_2 = -15.9$ ppb $a_3 = 2.8$ ppb $a_4 = -1.2$ ppb
SCIAMACHY ^e			
NH	13.7 ± 2.6	–	–
30° N–90° N	12.4 ± 8.0 ppb	–	–

^a Defined as $(\max - \min)/2$ of 2nd order Fourier fit to multi-annual monthly means of de-trended time series, see Fig. 9.

^b Describing the fitted intra-annual function $a_1 \cos(2\pi t) + a_2 \sin(2\pi t) + a_3 \cos(4\pi t) + a_4 \sin(4\pi t)$, see Fig. 9.

^c Retrieved with MIR-GBM v1.0, defined in Table 6.

^d Error for amplitude calculated from combining the standard errors (σ/\sqrt{n}) for the minimum (using March and April individual-year monthly means) and the maximum (August–October monthly means).

^e Retrieved with WFMD v2.0, numbers taken from Schneising et al. (2011, Table 3 therein).

Strategy for methane retrieval from the mid-IR FTIR network

R. Sussmann et al.

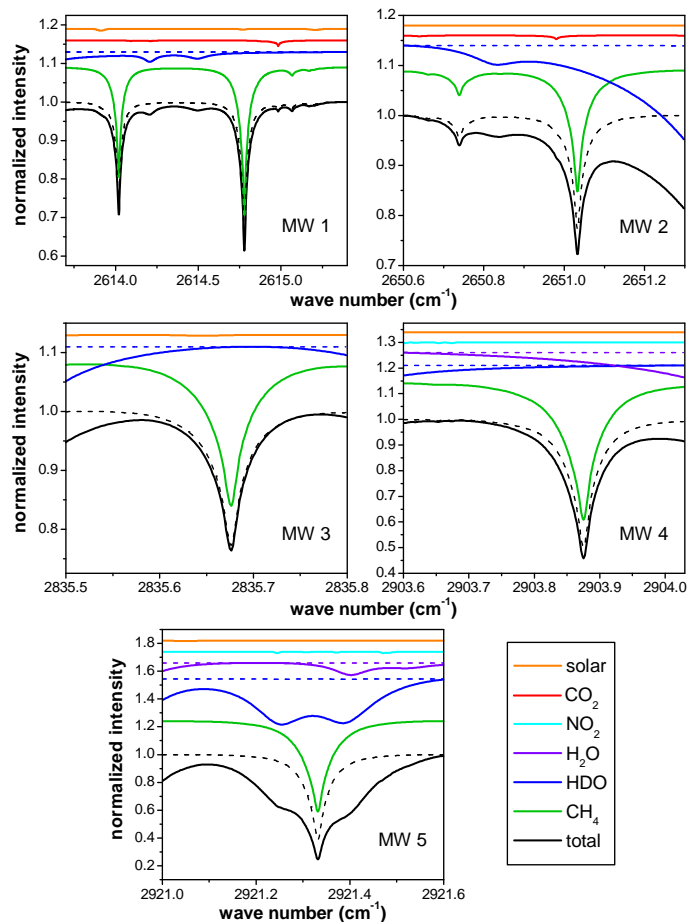


Fig. 1. Spectral contribution plot for a solar zenith angle of 65° . Solid lines are for a H_2O column of 44.9 mm (Wollongong maximum); dashed lines correspond to a H_2O column of 0.2 mm (Zugspitze minimum).

Title Page

Abstract

Introduction

Conclusions

References

Tables

Figures

◀

▶

◀

▶

Back

Close

Full Screen / Esc

Printer-friendly Version

Interactive Discussion



Strategy for methane retrieval from the mid-IR FTIR network

R. Sussmann et al.

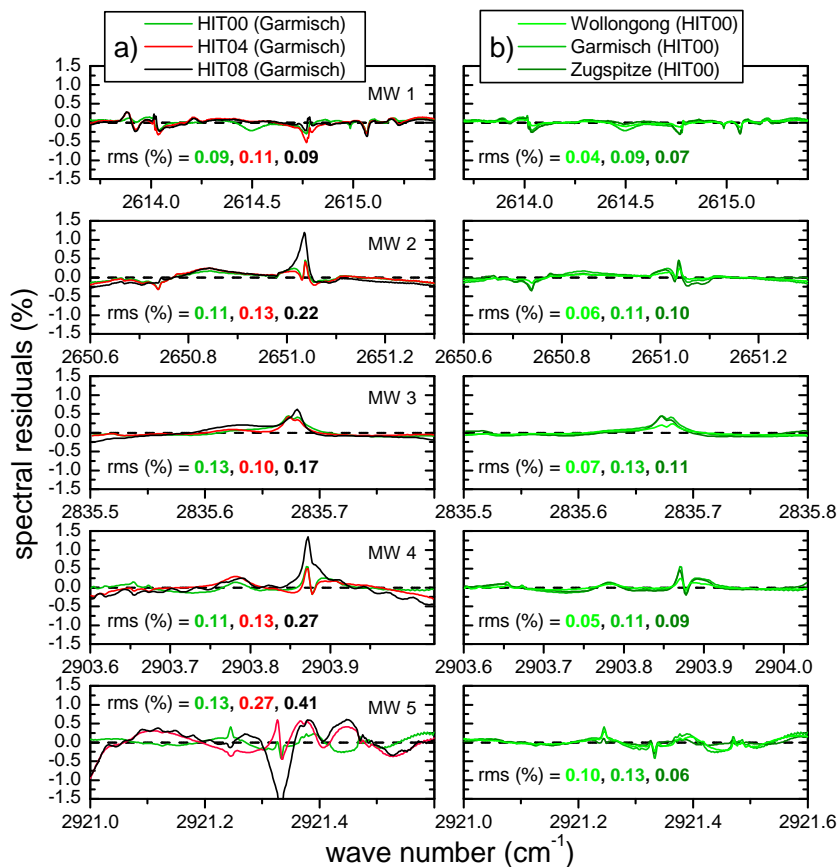


Fig. 2. (a) Averaged residuals (measured minus calculated) for the station Garmisch using HITRAN 2000 versus HITRAN 2004, and HITRAN 2008. (b) Averaged residuals using HITRAN 2000 shown for the 3 different stations Wollongong, Garmisch, and Zugspitze.

Title Page

Abstract

Introduction

Conclusions

References

Tables

Figures

◀

▶

◀

▶

Back

Close

Full Screen / Esc

Printer-friendly Version

Interactive Discussion



Strategy for methane retrieval from the mid-IR FTIR network

R. Sussmann et al.

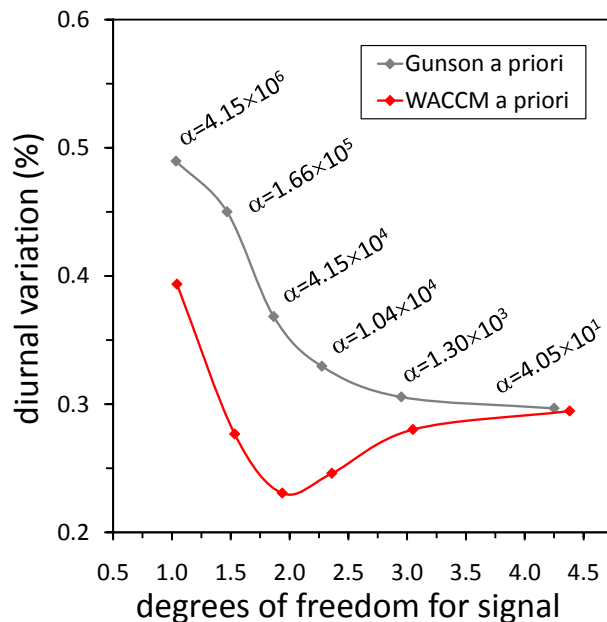


Fig. 3. Diurnal variation (1σ) of Tikhonov L_1 retrievals of Garmisch CH_4 columns as a function of information content (dofs). Corresponding numbers for the regularization strength α are indicated in black (using a diagonal measurement covariance with a signal-to-rms-noise ratio of 500). Note also the effect from using a non-optimum a priori profile (Gunson).

Strategy for methane retrieval from the mid-IR FTIR network

R. Sussmann et al.

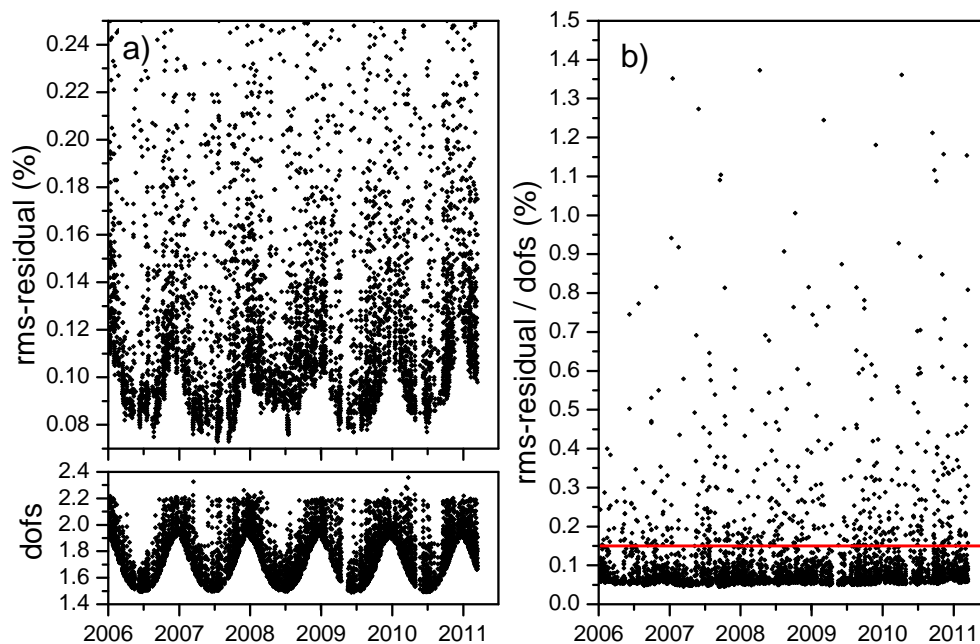


Fig. 4. (a) Upper trace: time series of spectral residuals from spectral fitting all 5 candidate micro windows together for the Garmisch site; lower trace: resulting degrees of freedom for signal (dofs). (b) Ratio of spectral residuals and dofs. Red line: quality selection threshold.

[Title Page](#)[Abstract](#)[Introduction](#)[Conclusions](#)[References](#)[Tables](#)[Figures](#)[◀](#)[▶](#)[◀](#)[▶](#)[Back](#)[Close](#)[Full Screen / Esc](#)[Printer-friendly Version](#)[Interactive Discussion](#)

Strategy for methane retrieval from the mid-IR FTIR network

R. Sussmann et al.

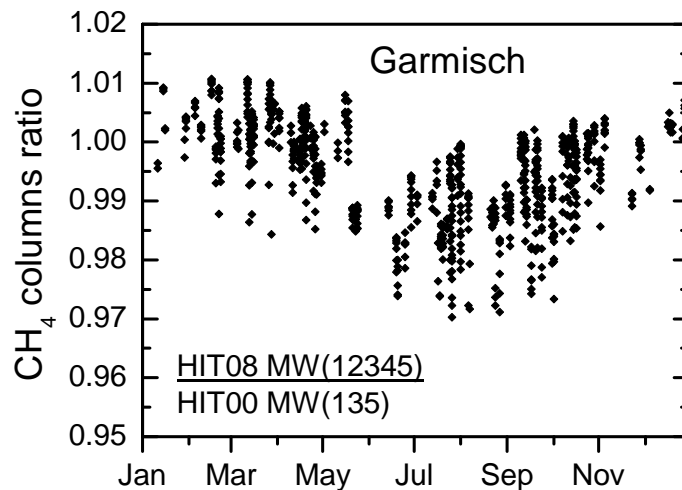


Fig. 5. Ratio of one year of Garmisch year 2007-methane retrievals with two differing retrieval strategies, i.e., using all 5 candidate micro windows and HITRAN 2008 (HIT08 MW(12345)) versus using only micro windows number 1, 3, and 5, and HITRAN 2000 (HIT00 MW(135)) plotted as a time series.

[Title Page](#)[Abstract](#)[Introduction](#)[Conclusions](#)[References](#)[Tables](#)[Figures](#)[◀](#)[▶](#)[◀](#)[▶](#)[Back](#)[Close](#)[Full Screen / Esc](#)[Printer-friendly Version](#)[Interactive Discussion](#)

Strategy for methane retrieval from the mid-IR FTIR network

R. Sussmann et al.

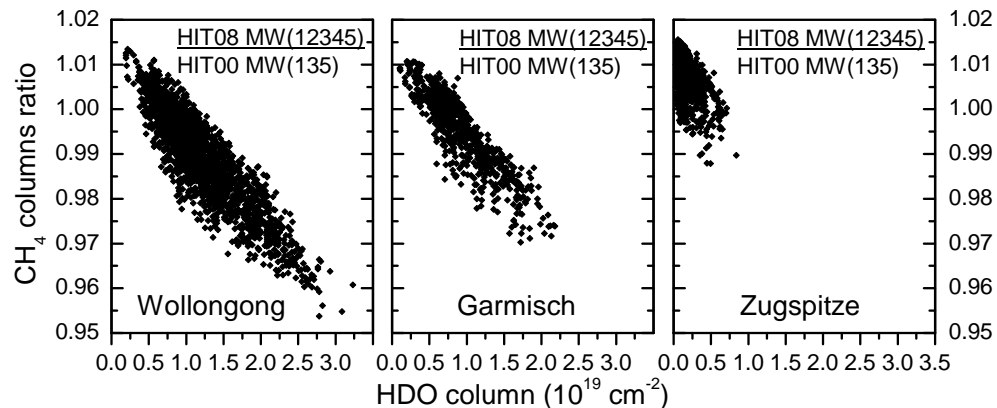


Fig. 6. Investigation of the seasonal artifact shown in Fig. 5: ratio of about one year of methane retrievals with two differing retrieval strategies as in Fig. 5, now plotted as a function of HDO column level for the 3 test sites (HDO columns are from the joint HDO retrieval of the HIT00 MW(135) run).

[Title Page](#)[Abstract](#)[Introduction](#)[Conclusions](#)[References](#)[Tables](#)[Figures](#)[⏪](#)[⏩](#)[◀](#)[▶](#)[Back](#)[Close](#)[Full Screen / Esc](#)[Printer-friendly Version](#)[Interactive Discussion](#)

Strategy for methane retrieval from the mid-IR FTIR network

R. Sussmann et al.

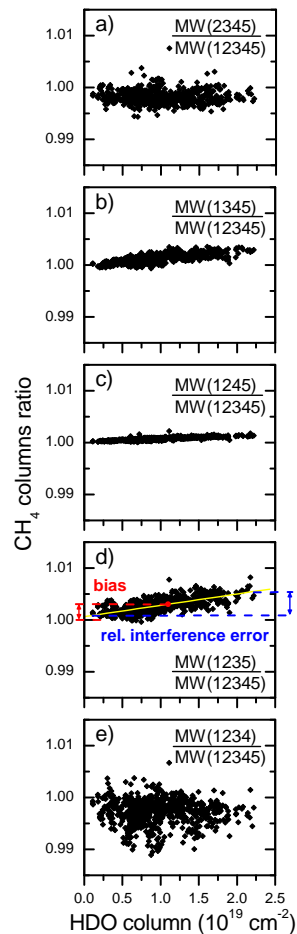


Fig. 7. Ratio of Garmisch year-2007 retrievals of columnar methane with one MW out of 5 dropped (a–e) versus retrieval with all 5 MWs plotted as a function of HDO column level. HITRAN 2000 was used in all cases. The definition of total relative interference error and overall bias is indicated.

[Title Page](#)
[Abstract](#)
[Introduction](#)
[Conclusions](#)
[References](#)
[Tables](#)
[Figures](#)
[◀](#)
[▶](#)
[◀](#)
[▶](#)
[Back](#)
[Close](#)
[Full Screen / Esc](#)
[Printer-friendly Version](#)
[Interactive Discussion](#)


Strategy for methane retrieval from the mid-IR FTIR network

R. Sussmann et al.

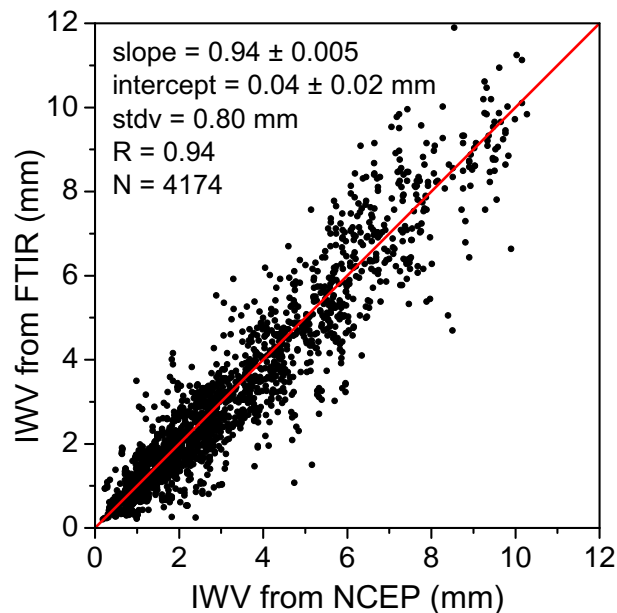


Fig. 8. Intercomparison of integrated water vapor (IWV) above the Zugspitze retrieved from the solar FTIR with the strategy of Sussmann et al. (2009) versus integrated water vapor profiles from NCEP. Four-times-daily NCEP profiles were interpolated to the times of the FTIR measurements.

Title Page

Abstract

Introduction

Conclusions

References

Tables

Figures

◀

▶

◀

▶

Back

Close

Full Screen / Esc

Printer-friendly Version

Interactive Discussion



Strategy for methane retrieval from the mid-IR FTIR network

R. Sussmann et al.

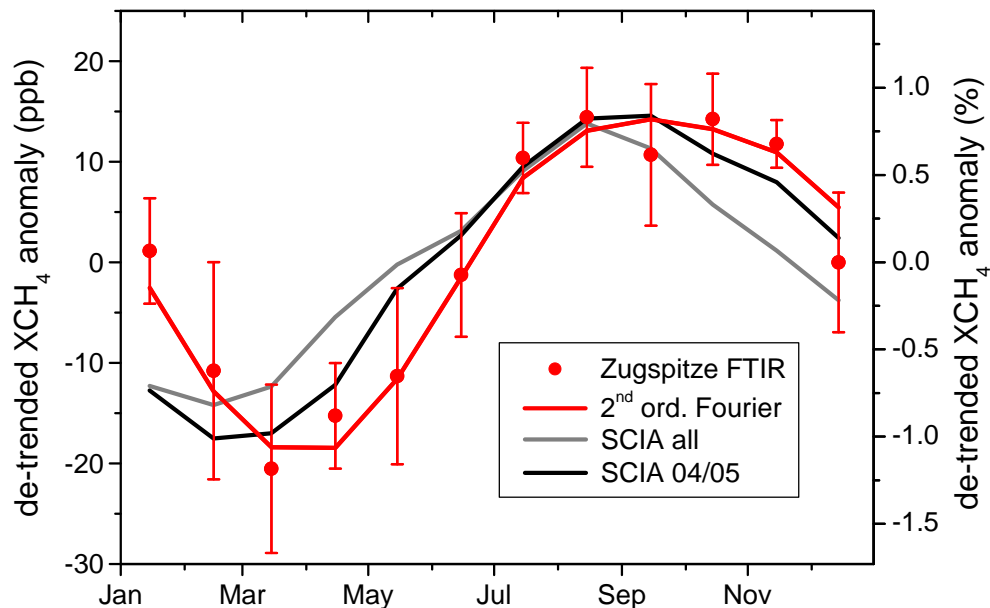


Fig. 9. Red points: multi-annual mean seasonality of column-averaged dry-air mole fractions of methane retrieved from Zugspitze FTIR. It has been derived from the de-trended monthly-mean time series in the interval (2004, 2009) with the retrieval strategy MIR-GBM v.1.0 (Table 8). Error bars are standard errors of the multi-annual monthly means for 95% confidence. Red line: fit of a 2nd order Fourier series. Grey line: seasonality derived from SCIAMACHY WFMDv2.0 data taken from Fig. 12 of Schneising et al. (2011) for the (2004, 2009) time interval. Black line: Same as grey line but using only SCIAMACHY (2004, 2005) data.

[Title Page](#)
[Abstract](#)
[Introduction](#)
[Conclusions](#)
[References](#)
[Tables](#)
[Figures](#)
[Back](#)
[Close](#)
[Full Screen / Esc](#)
[Printer-friendly Version](#)
[Interactive Discussion](#)

Strategy for methane retrieval from the mid-IR FTIR network

R. Sussmann et al.

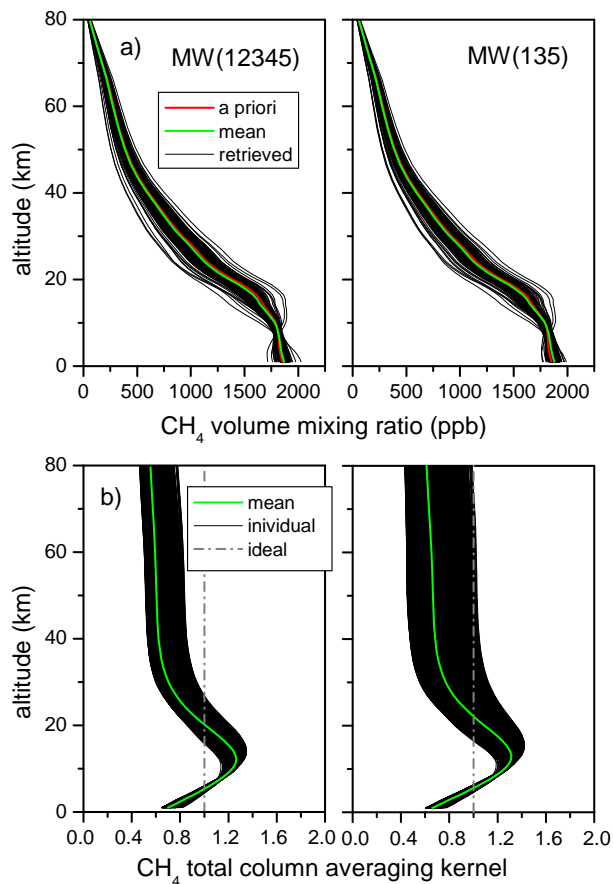


Fig. A1. (a) Ensembles of retrieved methane profiles using two differing micro window sets, i.e., MW(12345) and MW(135); HITRAN 2000 has been used in both cases. (b) Corresponding total-column averaging kernels.